Technical Report Documentation Page

1. Report No. FHWA/TX-09/0-6332-1	2. Government Accession No.	3. Recipient's Catalog No.
4. Title and Subtitle Phase 1 Report on the Development of Predictive Model for Bridge Deck Cracking and Strength Development		5. Report Date January 2009 6. Performing Organization Code
7. Author(s) Kevin J. Folliard, Phillip Pesek, Loukas Kallivokas, Kyle Riding, Anton Schindler		8. Performing Organization Report No. 0-6332-1
9. Performing Organization Name and Address Center for Transportation Research The University of Texas at Austin 3208 Red River, Suite 200 Austin, TX 78705-2650		10. Work Unit No. (TRAIS) 11. Contract or Grant No. 0-6332
12. Sponsoring Agency Name and Address Texas Department of Transportation Research and Technology Implementation Office P.O. Box 5080 Austin, TX 78763-5080		13. Type of Report and Period Covered Technical Report 9/2008 – 1/2009 14. Sponsoring Agency Code
15. Supplementary Notes Project performed in cooperation with the Texas Department of Transportation and the Federal Highway Administration.		

16. Abstract

Early-age cracking, typically caused by drying shrinkage (and often coupled with autogenous and thermal shrinkage), can have several detrimental effects on long-term behavior and durability. Cracking can also provide ingress of water that can drive chemical reactions, such as alkali-silica reaction (ASR) and sulfate attack. Because of the problems associated with cracking observed in bridge decks, and the impact of early-age cracking on long-term performance and durability, it is imperative that bridge decks be constructed with minimal early-age cracking and that exhibit satisfactory long-term performance and durability. To achieve these goals for bridges in the state of Texas, a research team has been assembled that possesses significant expertise and background in cement chemistry, concrete materials and durability, structural performance, computational mechanics (finite difference/element), bridge deck construction and maintenance, monitoring of in-site behavior of field structures, and the development of test methods and specifications aimed at practical implementation by state highway departments. This proposal describes a laboratory- and field-based research program aimed at developing a bridge deck cracking model that will ultimately be integrated into ConcreteWorks, a suite of software programs developed for TxDOT by this same research team.

17. Key Words Early-age cracking, drying shrinkage, bridge decks	18. Distribution Statement No restrictions. This document is available to the public through the National Technical Information Service, Springfield, Virginia 22161; www.ntis.gov.

19. Security Classif. (of report) Unclassified	20. Security Classif. (of this page) Unclassified	21. No. of pages 60	22. Price

Form DOT F 1700.7 (8-72) Reproduction of completed page authorized

PHASE 1 REPORT ON THE DEVELOPMENT OF PREDICTIVE MODEL FOR BRIDGE DECK CRACKING AND STRENGTH DEVELOPMENT

Kevin J. Folliard
Phillip Pesek
Loukas Kallivokas
Kyle Riding
Anton Schindler

CTR Technical Report:	0-6332-1
Report Date:	January 2009
Project:	0-6332
Project Title:	Development of Predictive Model for Bridge Deck Cracking and Strength Development
Sponsoring Agency:	Texas Department of Transportation
Performing Agency:	Center for Transportation Research at The University of Texas at Austin

Project performed in cooperation with the Texas Department of Transportation and the Federal Highway Administration.

Center for Transportation Research
The University of Texas at Austin
3208 Red River
Austin, TX 78705

www.utexas.edu/research/ctr

Disclaimers

Author's Disclaimer: The contents of this report reflect the views of the authors, who are responsible for the facts and the accuracy of the data presented herein. The contents do not necessarily reflect the official view or policies of the Federal Highway Administration or the Texas Department of Transportation (TxDOT). This report does not constitute a standard, specification, or regulation.

Patent Disclaimer: There was no invention or discovery conceived or first actually reduced to practice in the course of or under this contract, including any art, method, process, machine manufacture, design or composition of matter, or any new useful improvement thereof, or any variety of plant, which is or may be patentable under the patent laws of the United States of America or any foreign country.

Engineering Disclaimer

NOT INTENDED FOR CONSTRUCTION, BIDDING, OR PERMIT PURPOSES.

Project Engineer: Dr. David W. Fowler
Professional Engineer License State and Number: Texas No. 27859
P. E. Designation: Researcher

Acknowledgments

The research team would like to thank the TxDOT Project Director and Project Monitoring Committee for their support and assistance. Also, the team would like to thank the staff at the Concrete Durability Center.

Table of Contents

Chapter 1. Introduction and Scope 1

Chapter 2. Literature Review 3
2.1 Introduction 3
2.2 Volume Changes in Concrete 3
2.2.1 Plastic Shrinkage 3
2.2.2 Chemical and Autogenous Shrinkage 7
2.2.3 Drying Shrinkage 9
2.2.4 Thermal Deformations 9
2.2.5 Moisture Gradients 11
2.2.6 Carbonation Shrinkage 11
2.3 Development of Mechanical Properties 11
2.3.1 Factors Influencing Strength Development 12
2.3.2 Maturity 13
2.3.3 Compressive strength 13
2.3.4 Elastic Modulus 14
2.3.5 Tensile Strength 14
2.3.6 Creep and stress relaxation 14
2.4 Bridge Deck Cracking 15
2.4.1 Mechanisms of Bridge Deck Cracking 16
2.4.2 Bridge Deck Cracking in Texas 17
2.4.3 Prediction and Modeling 19

Chapter 3. Work Plan 21
3.1 Materials and Mixture Proportions 21
3.2 Laboratory Evaluations 22
3.2.1 Cracking Frames 22
3.2.2 Plastic shrinkage 29
3.2.3 Autogenous shrinkage 30
3.2.4 Drying shrinkage 31
3.2.5 Thermal effects 33
3.2.6 Creep and Stress Relaxation 36
3.3 Field Evaluations 38
3.4 Framework for Modeling Bridge Deck Cracking 38
3.5 Implementation and Training 43
3.6 Final Project Report 43
3.7 Information Technology (IT) Deliverables to TxDOT 44
3.8 Assistance or Involvement by TxDOT 44

References 45

List of Figures

Figure 2.1: Relationship between evaporation from concrete or mortar surface, compared to evaporation from free water surface (Al-Fadhala and Hover, 2001) 5
Figure 2.2: Test set-up to measure early-age tensile strength of concrete, consisting of (a) two-part mold and (b) support frame that mechanically separates one part of the mold from the other at desired time. 7
Figure 2.3: Time dependence of restrained shrinkage and creep (Mehta, 1993) 15
Figure 2.4: Causes of bridge deck cracking. 16
Figure 2.5: Typical precast, prestressed panel details 17
Figure 2.6: Typical stair step cracking. 18
Figure 2.7: Typical transverse cracking. 19
Figure 3.1: Rigid Cracking Frame Drawing (Riding 2007) 22
Figure 3.2: Photograph of Rigid Cracking Frame (Whigham 2005) 23
Figure 3.3: Free Shrinkage Frame a) Diagram and b) Photograph 24
Figure 3.4: Conceptual approach to overall cracking frame test set-up 25
Figure 3.5: Typical free shrinkage frame results (for mixture C1L) 27
Figure 3.6: Typical rigid cracking frame results (for mixture C1L) 27
Figure 3.7: Summary of boundary conditions affecting heat transfer to/from bridge deck 33
Figure 3.8: Photograph of instrumented bridge prior to deck placement 34
Figure 3.9: Temperature development in bridge deck at mid-depth, above, and between girders (Riding et al. 2009) 35
Figure 3.10: Vertical temperature profile in the bridge deck between girders (Riding et al. 2009) 35
Figure 3.11: Stress development of various bridge deck mixtures (Riding et al. 2009) 36
Figure 3.12: A simple span bridge deck exposed to temperature differentials on its vertical sides; longitudinal normal stress distribution, sampled at 2 hour intervals during the first 8 hours from the onset of the thermal gradients. 43

List of Tables

Table 3.1: Materials to be included in laboratory evaluations 21
Table 3.2: Completed Testing Matrix for IAC on Impact of Fly Ash on Shrinkage Cracking 25
Table 3.3: Summary of Cracking Frame Results for IAC Study 26
Table 3.4: Cracking Frame Testing Matrix for This Project 28
Table 3.5: Software features currently available within ConcreteWorks for each concrete member type (with bridge decks in bold) (Riding 2007) 39
Table 3.6: Proposed bridge deck cracking model (with newly proposed features in shaded cells) 40

Chapter 1. Introduction and Scope

This report summarizes the findings of Phase I of TxDOT Project 0-6332, "Development of Predictive Model for Bridge Deck Cracking and Strength Development." Specifically, this report presents a concise summary of research performed to date related to volume changes in concrete and resultant stresses in bridge decks, identifies research needs related to these issues, and sets forth a work plan for Phase II of this project.

For informational purposes, this project is 3-year project, starting September 2008 and ending August 2011. The research team is led by Dr. Kevin Folliard (PI) and includes Drs. Loukas Kallivokas (UT-Austin), Dr. Anton Schindler (Auburn University), and Dr. Kyle Riding (Kansas State University). The main objectives of this project are to:

- Identify and evaluate the factors influencing the early-age cracking of bridge decks.
- Integrate key findings into ConcreteWorks, a software program previously developed by this research team for TxDOT under Project 4563.

This project is divided into the following Phases and Tasks:

Phase I
Task 1 – Literature Review
Task 2 – Development of Framework for Bridge Deck Cracking Model
Task 3 – Development of Draft Testing Matrix for Phase II
Task 4 – Phase I Summary Report

Phase II
Task 5 – Laboratory Evaluations
Task 6 – Field Evaluations
Task 7 – Model Development, Calibration, and Validation
Task 8 – Implementation and Training
Task 9 – Final Project Report

This report satisfies the requirements for Task 4 (Phase I Summary Report) and includes a concise literature review (related to bridge deck cracking), describes how a bridge deck cracking module will be developed and integrated into ConcreteWorks, and presents a draft testing matrix for Phase II laboratory and field evaluations.

Chapter 2. Literature Review

2.1 Introduction

Durability issues have plagued the state of Texas for some time, with distress caused by alkali-silica reaction (ASR), delayed ettringite formation (DEF), and corrosion of reinforcing steel. All of these distress mechanisms are driven by the need for water (moisture) and corrosion is fueled by chlorides that diffuse into concrete with the entering water. As such, any process that increases the rate at which water (and its entities) enters concrete can help to exacerbate these problems. It is for this primary reason that this project is aiming to prevent or minimize bridge deck cracking, thereby prolonging the service life of a structural component that is subject to everything from rain to snow to deicing salts to abrasion, and whose premature failure can especially drive corrosion, ASR, and DEF.

Bridge deck cracking has been found to be a serious threat to America's aging infrastructure, having earned a grade of D in a 2009 Progress Report by the American Society of Civil Engineers. Prior to this rating, a survey of state transportation departments found that more than 100,000 bridge decks had exhibited early-age transverse cracking (Krauss and Rogalla, 1996). The multi-mechanistic nature of bridge deck cracking, and the fact that the mechanisms interact and influence each other, make bridge deck cracking a difficult issue to understand or predict.

This concise literature review will attempt to highlight some of the factors involved in bridge deck cracking, explain the volume changes that cause cracking, and describe the development of concrete properties (strength, modulus, etc.) that resist early-age cracking. It is not meant to be an exhaustive discussion of all that is known on volume changes, mechanical development, and bridge deck cracking, but rather a synthesis of the knowledge that will be necessary for completion of a study on bridge cracking. Many journal and conference papers, full chapters, and even full books have been devoted to early-age cracking, and the research team has been active in this area for several years. The goal of this review is simply to describe the basic mechanisms of volume change (plastic, autogenous, thermal, etc.), to describe how these volume changes can lead to cracking, and to highlight research needs that will be addressed in the current project.

2.2 Volume Changes in Concrete

Concrete is a dynamic material, one whose microstructure changes with time and one whose volume will change from the early stages of hydration to the later stages of service life. This section briefly describes the most relevant forms of volume change that affect concrete, in general, and bridge decks, in particular.

2.2.1 Plastic Shrinkage

Plastic Shrinkage occurs as water is lost to the environment while the concrete is still plastic (e.g. prior to setting). Plastic shrinkage cracking can occur in bridge decks or other elements with high surface/volume ratios once the cumulative evaporation from the concrete surface exceeds the cumulative bleeding of the concrete. When cumulative evaporation exceeds cumulative bleeding, water is drawn from within the bulk of the concrete, and the concrete goes into tension—unfortunately, it does so at a time when its tensile strength is negligible. To

understand and better yet, to prevent plastic shrinkage cracking, one must know and take into account the bleeding rate (and capacity), evaporation rate (function of surrounding environment, as well as the temperature at the surface of the concrete, and early strength development. Unfortunately, as described next, most practitioners only take into account one of these governing factors, namely the evaporation rate from the surface of the concrete.

The current approach advocated by ACI (ACI 305-96), and followed by many agencies and highway departments, is to calculate the evaporation rate using Menzel's equation (in the form of the oft-used ACI nomograph that predicts evaporation rate based on concrete temperature, ambient temperature, wind speed, and relative humidity). However, this approach is lacking in that Menzel's equation is not particularly accurate for concrete applications. This is because it was based on predicting evaporation rate from a reservoir of water. The evaporation rates calculated from the ACI nomograph are also highly dependent on where the input information was obtained from. While the specifications in the chart call for readings taken 20 in. from the concrete surface, environmental conditions (i.e. wind speed, relative humidity, and temperature) are evaluated several feet to several hundred feet from the concrete surface. Concrete temperatures, usually only checked one time when slump tests are performed, vary greatly after the concrete has been poured. These discrepancies can lead to erroneous values from the nomograph, providing an evaporation rate that is not only inaccurate due to the fact that the nomograph does not properly model concrete, but also from the fact that environmental inputs were not taken as specified. Hover (2006) found that the difference between accurate and inaccurate chart inputs could cause significant changes in the predicted evaporation rates. Furthermore, this approach of solely quantifying evaporation rates neglects the key role of bleeding (rate and amount) and does not address the other side of the equation, namely the early tensile strength of concrete that must resist the stresses generated by plastic shrinkage.

As previously stated, the ACI nomograph, based on Menzel's equation was originally developed for the estimation of evaporation from a free water surface (Lake Hefner in Oklahoma) and not from the top surface of concrete. Given the relevance of plastic shrinkage cracking to bridge decks, especially in regions of Texas that are quite windy (e.g. Lubbock), this traditional approach will not suffice. Dr. Folliard performed research with Dr. Kenneth Hover of Cornell University in 1989 focusing on this very issue, and it was found that the rates of evaporation from free water (or "pan" evaporation) differed considerably from the actual rates of evaporation from fresh concrete. In subsequent research, Al-Fadhala and Hover (2001) proposed a relationship between the evaporation rate from the surface of concrete or mortar and the evaporation of water from a free surface (Figure 2.1). The current version of ConcreteWorks uses the modification to Menzel's equation that were proposed by Al-Fadhala and Hover (2001), but this modification is based on a somewhat limited database—more research is needed to develop a more robust approach to estimating evaporation rates.

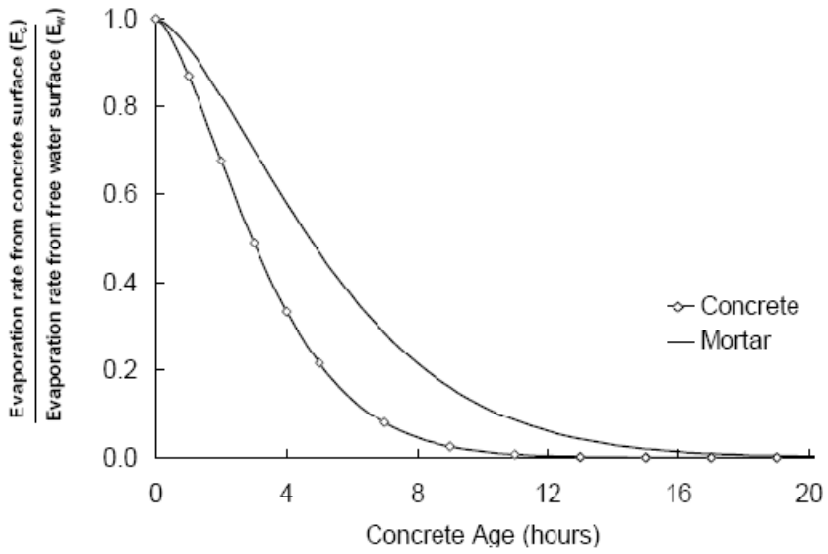

Figure 2.1: Relationship between evaporation from concrete or mortar surface, compared to evaporation from free water surface (Al-Fadhala and Hover, 2001)

As just described, research is needed to more accurately predict evaporation rates from concrete surfaces, in general, and bridge decks specifically. To undergo evaporation, bleed water must first reach the surface of concrete to evaporate; yet, bleeding rate and capacity are almost never considered when practitioners are evaluating the risk of plastic shrinkage cracking. Surprisingly, very few studies have attempted to quantify the bleeding rate of concrete mixtures. Powers (1968) reported bleeding rates of 0.24 to 0.83 lb/ft^2/hr, and noted that "in all cases the period of constant rate lasts 15 to 30 minutes at the most and thereafter the rate diminishes, reaching zero within an hour and a half." Ono (1996) suggests that Power's data was the underpinning for the ACI recommendation that preventive measures against plastic shrinkage cracking should be taken when evaporation rates exceed 0.20 lb/ft^2/hr as this would represent a conservative lower-bound value above which the evaporation rate would exceed the bleeding rate. However, as previously noted, this approach of specifying a single threshold value for evaporation rate is clearly flawed as it ignores the bleeding rate and tensile strength development of concrete. Hover (2006) calls attention to the fact that most of today's concrete mixtures incorporate slag, fly ash, silica fume, high cement contents, fine cements, or water reducers that can create a variety of bleeding rates, with many falling below 0.2 lb/ft^3/ hr. Clearly, more research is needed to quantify bleeding rates and capacities (based on materials, mixture proportions, temperature, etc.) and to integrate these data with evaporation rates from actual concrete surfaces in order to estimate the time at which stresses begin to develop. Thereafter, it is important to estimate the tensile strength development to determine whether tensile stresses due to plastic shrinkage or early tensile strength "win the battle."

In order to define the time before which plastic shrinkage is a significant concern and define the point in time in which tensile strength begins to develop, it becomes important from a practical (and technical) perspective to know when concrete sets. A setting time model, which uses standard inputs from semi-adiabatic calorimetry (as defined in Eq. 1), was developed by Schindler (2004) to predict the initial and setting times of concrete, respectively. This approach

is especially useful nowadays as more and more practitioners and researchers are developing heat of hydration parameters for their concrete mixtures.

ASTM C 403 Initial set:

$$t_{ei} = \tau \cdot \left(-\ln\left[\frac{0.14 \cdot w/cm}{\alpha_u} \right] \right)^{\frac{-1}{\beta}} \quad \text{Eq. 1}$$

ASTM C 403 Final set:

$$t_{ef} = \tau \cdot \left(-\ln\left[\frac{0.26 \cdot w/cm}{\alpha_u} \right] \right)^{\frac{-1}{\beta}} \quad \text{Eq. 2}$$

where, t_{ei} = equivalent age at initial set (hours),
t_{ef} = equivalent age at final set (hours), and
w/cm = water-cementitious materials ratio.

Another key input into the proposed plastic shrinkage cracking model is the rate of tensile strength development as it is this strength that must resist the tensile stress developed by plastic shrinkage. This is not a trivial property to measure as it is very difficult to quantify tensile strength development during the timeframe in which plastic shrinkage is a concern. Conventional methods are not feasible as test cylinders are too fragile to strip and test. An innovative testing method has been developed by Abel and Hover (1989), as shown in Figure 2.2. This apparatus consists of a two-part mold into which fresh concrete is placed. A series of specimens are cast for each mixture (typically six to nine), and at desired early-age time intervals, the movable frame separates one half of the mold from the other, with a load cell used to measure the tensile stress at failure.

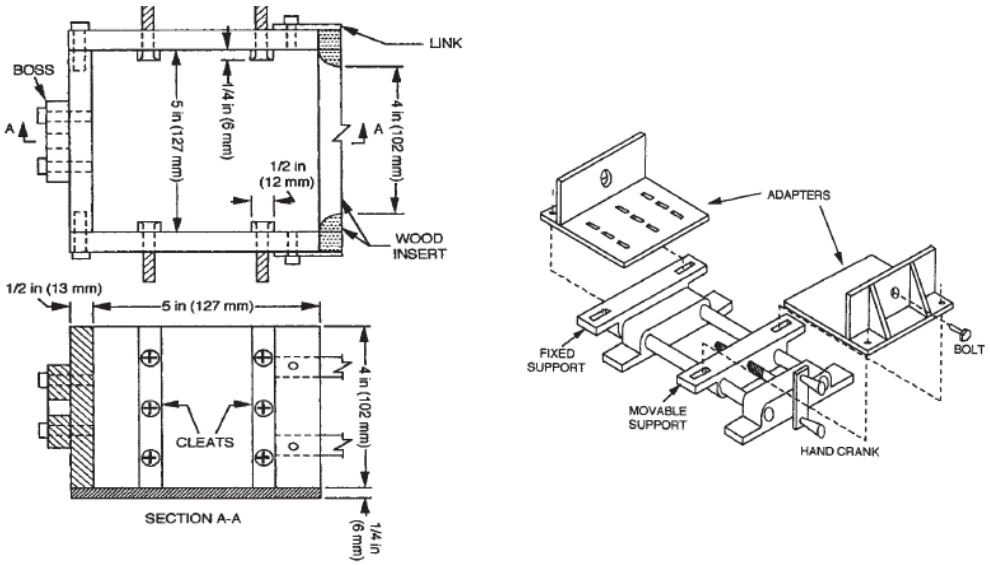

Figure 2.2: Test set-up to measure early-age tensile strength of concrete, consisting of (a) two-part mold and (b) support frame that mechanically separates one part of the mold from the other at desired time.
A load cell directly measures the tensile stress required to fail the specimen.

In summary, plastic shrinkage cracking is a significant concern for concrete flatwork, including bridge decks, especially in areas such as Lubbock, where evaporation rates are typically quite high. As previously mentioned, the basic mechanisms of plastic shrinkage cracking are fairly well understood, and there is information in literature (and specifications) on how to deal with singular aspects of this phenomenon, such as rate of evaporation. However, to date, there has not been an implementable approach or model to predict plastic shrinkage cracking in concrete, in general, or bridge decks, specifically. However, practitioners have learned to appreciate the conditions that most often lead to plastic shrinkage cracking—hot, windy, dry days that increase the rate of evaporation. Practitioners have also learned that when placing concrete with SCMs, it is essential to take interim steps to ensure that the top surface above a concrete slab has moisture available to it through the use of fog misters, especially when silica fume is used. In addition, the use of synthetic fibers has become very common as a safeguard against plastic shrinkage cracking. Although there remains a question about the specific manner by which fibers may help prevent cracking, it has been proposed that the higher early tensile strength and strain capacity and/or the increased rate of bleeding imparted by discontinuous fibers are quite beneficial.

2.2.2 Chemical and Autogenous Shrinkage

In recent years, there has been considerable interest in early-age behavior of concrete, and much of this interest has been fueled by the use of high-performance concrete (HPC), which is often characterized by relatively low water-to-cementitious materials ratio (w/cm) of less than 0.40 and the use of supplementary cementing materials. When using such mixtures in field

applications, it is important to realize that there may be insufficient water present internally to fully hydrate the portland cement. As the cement hydration proceeds and the amount of free water decreases, air takes the place of water in pores, lowering the pore relative humidity. An air-water meniscus forms with an accompanying surface tension. The surface tension imparts a tensile stress on the matrix, causing shrinkage. This is referred to as "chemical shrinkage," which is defined as the volume reduction associated with the hydration reactions in a cementitious material (Jensen and Hanson, 2001). When aggregates are present, they are placed in compression by the cement matrix, providing restraint. The degree of restraint that the aggregates provide depends on the aggregate stiffness and percent volume (Riding, 2007).

Although they are often considered to be the same property, autogenous shrinkage is different from chemical shrinkage in that it is defined as the bulk strain of a closed, isothermal, cementitious material system not subjected to external forces. Chemical shrinkage can then be defined as "a change in the absolute volume," while autogenous shrinkage can be defined as "a change in the apparent volume" (Jensen and Hansen, 2001). These two quantities tend to be identical up until concrete sets; thereafter, they deviate, with chemical shrinkage typically being significantly larger than autogenous shrinkage.

Researchers at UT-Austin have been very active in research related to both chemical and autogenous shrinkage and are well versed in standard and non-standard test methods aimed at quantifying these early-age volume changes. However, it should be noted that at this point, chemical and autogenous shrinkage is generally only a concern for concrete with w/cm below about 0.40-0.41, and that most bridge decks in Texas are cast at w/cm at or above these w/cm values (note the maximum allowable w/cm for bridge decks in Texas is 0.45). As such, autogenous shrinkage may not be a major concern for bridge decks, compared to concrete cast at lower w/cm values (e.g., precast elements). The current version of ConcreteWorks utilizes a locally calibrated version of the model developed by Hedlund to reduce the w/cm at which autogenous shrinkage develops, the time at which autogenous shrinkage begins, and does not include the temperature modification term. The ultimate autogenous shrinkage value used on concrete works is calculated using Eq. 3:

$$\varepsilon_{ault} = (-0.94 + 2.238 * {}^{w}/_{cm}) * 10^{-3} \quad \text{Eq. 3}$$

The w/cm at which autogenous shrinkage develops in ConcreteWorks is 0.42, which corresponds to the theoretical w/cm at which complete hydration is possible (Mindess, Young, and Darwin, 2003). Additionally, autogenous shrinkage begins at the virtual time-of-set, not at 24 equivalent age hours as in the Hedlund model. Eq. 1 will be used at the beginning of the proposed bridge deck cracking model, with the expectation that changes will be made as data is generated through project findings. This assumption is predicated on previous work done by Jensen and Hansen (2001), Laura et al (2001), and others, that has shown that a clear relationship exists between internal relative humidity and autogenous shrinkage, demonstrating that self-desiccation induced by chemical shrinkage leads directly to internal shrinkage.

There have been various studies in recent years aiming to combat autogenous shrinkage with shrinkage-reducing admixtures, saturated lightweight aggregates, and super-absorbent polymers (Folliard and Berke, 1997; Bentz and Jensen, 2004; Bentz, 2006). Given that concrete used in Texas bridge decks do not typically suffer significantly from autogenous shrinkage (due to w/cms being in the range of 0.40 to 0.45), it remains to be seen whether such measures are essential to help minimize early-age cracking.

2.2.3 Drying Shrinkage

Shrinkage caused by water loss from concrete has long been recognized as a cause of cracking of bridge decks and other flatwork. Although drying shrinkage has been somewhat overshadowed in recent years by concerns about autogenous shrinkage, it remains a major concern in the concrete industry. Mechanistically, the driving force behind drying shrinkage, namely the loss of internal water to the environment, is identical to the underlying cause of plastic shrinkage, the only difference being the nominal cut-off point in time when concrete transitions to a solid material (i.e. setting time). When water is lost from concrete, water is lost first from the largest pores, as the water in these pores is held with the least binding energy; water is then lost from smaller and smaller pores, with pores below 50 nm being most responsible for drying shrinkage. As such, data on pore size distributions of the paste phase can be helpful in predicting shrinkage potential. The capillary stress theory, captured by the Kelvin/Laplace-Gibbs equation (Eq. 4), can be used to estimate the resultant stresses triggered by water loss as a function of pore size radius (r) and surface tension (γ) of the pore water.

$$\sigma = {}^{2\gamma}/_{r} \qquad \text{Eq. 4}$$

Various factors, such as w/cm, paste content, water content, cement type and fineness, SCM (dosage and type), chemical admixtures, aggregate type, and aggregate content affect the rate of shrinkage development and ultimate magnitude of shrinkage. One can optimize the pore size distribution to minimize the potential for drying shrinkage and shrinkage-reducing admixtures (SRAs) can be used to reduce the surface tension of the pore water (Folliard and Berke, 1997).

In field structures, factors such as curing method and regime, environmental conditions (temperature, RH, etc.) and surface/volume ratio of the structural elements play major roles in determining drying shrinkage behavior. For bridge decks, drying occurs from the top down, and as such, moisture gradients develop which can generate significant stress gradients, with the highest stress at the top of the deck.

There have been literally hundreds of studies on the drying shrinkage of concrete, evaluating everything from materials to mixture proportions to curing conditions. Because of this large database of shrinkage data, there have been several attempts to quantify and predict drying shrinkage as a function of time, including the following models: ACI 209, CEB 90, B3, and GL 2000. Al-Manaseer and Lam (2005) recently evaluated these four models from a statistical perspective. Although there is no clear consensus on which of these models is the best for predicting shrinkage (and/or creep), the B3 model (developed by Bazant and included in RILEM recommendations) is the most recent model and has been favored by researchers and practitioners in recent years.

2.2.4 Thermal Deformations

While thermal deformations are usually thought of as a problem for mass concrete, the affects of thermal shrinkage must also be considered for bridge deck systems. Due to heat released from hydration reactions, concrete temperature will rapidly increase after concrete placement (given typical environmental conditions). After approximately 24-hours have passed, the concrete temperatures start to decrease as heat loss to the environment becomes greater than

the heat generated from the hydration reactions. After several days have passed, the concrete heat production will nearly stop, and the concrete system will assume thermal behavior based on heat transfer with the surrounding environment. Although bridge decks usually do not crack due to thermal shrinkage alone, it must be realized that these strains are placed on top of drying (and autogenous) shrinkage strains that are occurring during the same time period (Babaei and Fouladgar, 1997).

In order to predict the strains associated with the thermal changes taking place at early ages, a model was developed under TxDOT 4563 to predict the temperature development of the concrete based on the progression of hydration reactions. Dr. Folliard's research group at UT-Austin has developed perhaps the most extensive heat of hydration database ever assembled over the past six years. This database, populated by isothermal and semi-adiabatic calorimetry data, has led to the development of hydration models for concrete mixtures containing a wide range of cement types, SCM types and dosages, and chemical admixtures types and dosages (Poole, 2007; Riding, 2007). The models generated were based on both Bogue's and Rietveld analyses and were aimed at developing predictive models for quantifying the progress of hydration through the use of Eq. 5:

$$Q_h(t) = H_u * W_c * \left(\frac{\tau}{t_e}\right)^{\beta} * \left(\frac{\beta}{t_e}\right) * \alpha(t_e) * \exp\left(\frac{E_a}{R}\left(\frac{1}{273+T_r} - \frac{1}{273+T_c}\right)\right) \quad \text{Eq. 5}$$

where Q_h= rate of heat generation (W/m^3), H_u = total heat available (J/kg), and W_c = cementitious materials content (kg/m^3).

Equations for H_u are available in literature, but a more accurate equation is presented in Poole (2007). E_a, the apparent activation energy, describes the isothermal calorimetry testing that was developed to describe the effects of w/cm, cement chemistry, SCMs, and chemical admixtures on the E_a of portland cement pastes. The model is also discussed in detail in work done by Poole (2007). The parameters α, τ, and β model the shape of the hydration curve from semi-adiabatic calorimetry. The model shown in Eq. 5 is based on a range of concrete mixtures that are typically used in mass concrete, bridge decks, and precast elements. Under TxDOT 4563, a finite difference-based model was developed to incorporate the heat of hydration models into field structures and to then apply advanced heat transfer principles to generate spatial, time-temperature histories throughout hydrating field elements, including mass concrete elements, bridge decks, and precast girders (Riding, 2007). This model takes into account a wide range of boundary conditions, including solar radiation, convection, irradiation, and other mechanisms, and accounts for practical field issues such as curing conditions and formwork type and removal age. The model integrated into ConcreteWorks includes weather files for 239 cities from across the United States and includes data on temperature, relative humidity, wind speed, solar radiation, cloud cover, etc. The heat generation and transfer models have been calibrated and validated with well over 35,000 hours of field data from mass concrete placements, but only minimal field validation was performed under TxDOT 4563 for bridge decks.

Other thermal issues that must be accounted for when modeling a bridge deck include thermal conductivity, specific heat, and coefficient of thermal expansion, all of which are already dealt with in the ConcreteWorks module for heat generation and transfer in bridge decks. ConcreteWorks, however, is lacking in that it does not address the fact that coefficient of thermal expansion is affected by the moisture content (internal relative humidity) of concrete (Emmanuel

and Husley, 1977). When typical concrete mixture proportions are used, the CTE of concrete in the partially dry state can be as much as 15% more than in the CTE in the saturated state.

2.2.5 Moisture Gradients

As mentioned previously, bridge decks will be subjected to drying conditions that will impart a moisture gradient within the deck. This moisture gradient will trigger warping effects in the deck. A variety of detailed laboratory studies and modeling efforts have addressed this issue (Wittman and Roelfstra, 1980; Akita et al. 1997; Bentz et al. 1998; Grasley et al. 2004), although each has focused on laboratory testing under controlled conditions rather than realistic field conditions. Moisture gradients were not accounted for in the mass concrete crack prediction model in ConcreteWorks, as this is a minor issue at early-ages in such elements when compared to thermal effects. However, it is quite clear that moisture gradients must be predicted and the implications of such gradients in terms of shrinkage strains and warping must be integrated into models aimed at predicting bridge deck cracking.

2.2.6 Carbonation Shrinkage

Though not commonly thought to be a problem in bridge deck durability, carbonation shrinkage has the ability to reduce concrete surface strength and induce differential shrinkage in concrete elements. In carbonation shrinkage, cement paste (all hydration products, starting with CH) will react with carbon dioxide, lowering the pH of the system (and hence causing corrosion if carbonation front reaches steel) and resulting in shrinkage in the carbonated layer. Generally, this is usually not a major concern in high-quality concrete, as carbonation typically does not penetrate more than 0.5 in. into the concrete surface. If poor quality concrete is made, or if reinforcing steel is not provided with adequate cover, then carbonation shrinkage may affect a deeper section of the concrete, and corrosion of the rebar may take place (ACI 224R, 2001). Carbonation shrinkage also requires a specific range of relative humidity in the concrete; enough to provide essential water for carbon dioxide transport, but not so high that the pore structure is saturated and carbon dioxide cannot move through the saturated pores. A relative humidity of 50% produces the greatest values of carbonation shrinkage (Mindess, Young, and Darwin, 2003). While carbonation shrinkage and resulting corrosion of steel are possible in bridge decks, it is not a common issue. The necessary environmental conditions, the low permeability of carbon dioxide into concrete, and the fact that carbonation profiles rarely exceed the cover depth for reinforced structures make carbonation a minor issue in bridge deck durability.

2.3 Development of Mechanical Properties

In attempting to understand the many factors and forces involved in bridge deck cracking, one must be aware of the mechanical properties of a given bridge deck system. Obtaining a full understanding of how strength development, modulus development, and the mechanisms of creep resist the buildup of tensile stresses is integral in attempting to accurately predict the cracking potential of a bridge deck system.

While it is very important to have an understanding of the failure-inducing stresses that can build up in a concrete structure, no real progress can be made unless one has a firm grasp of the concrete strength development that works to resist the stresses. Since the rate of strength development is a temperature dependent property, maturity methods are needed to calculate the development of mechanical properties. One should also have a general feel for how different

factors, such as the water to cementitious products ratio (w/cm), use of supplementary cementitious materials (SCMs), and aggregate type and gradation, play a role in the long and short-term strength development of concrete. Finally, understanding the empirical relationships between compressive strength, tensile strength, modulus of elasticity development, and the development of creep behavior will allow the researcher to predict the concrete's ability to resist tensile stress over time.

2.3.1 Factors Influencing Strength Development

Several factors can have effects on the development of compressive and tensile strength. Water/cement ratio is commonly used as the main predictor for concrete strength, with high w/cms producing lower strength concrete, and higher w/cms producing stronger concrete. This is primarily achieved through the reduction in capillary porosity within the concrete. Lower w/cms also result in a faster strength development rate than high w/cm mixtures. Testing done by Abel and Hover on concrete 2-8 hours old showed faster tensile strength development, lower deformation at failure, and higher tensile strengths with lower w/cms. These findings are especially relevant to bridge decks, representing the concrete behavior and stresses during which plastic shrinkage cracking usually occurs (Abel and Hover, 1998). At different w/cms, one must also consider the chemical and physical properties of the cement being used. The levels of C_3S and C_2S are the primary chemical components in influencing long and short term strength of portland cement concrete, with C_2S contributing to long-term strength and C_3S contributing to short-term strength. Focus must also be paid to the fineness of the cement being used, with high percentages of particles under 3μm resulting in high 1-day strength and high percentages of 3-30μm particles resulting in higher 28-day strength (Mindess, Young, and Darwin, 2003).

Use of SCMs can also play a large role in determining the strength of concrete. In general, pozollanic admixtures, such as Class F fly ash, slow the rate of early-age strength gain, but increase the strength of concrete at later ages. These products affect strength by reacting with the weaker cement hydration products (CH) to produce strong components (C-S-H). SCMs, such as silica fume, can also increase concrete strength by reducing the capillary porosity and increasing the strength between coarse aggregates and surrounding mortar. Pozzolans will decrease the porosity at the interfacial transition zone, effectively strengthening the common point of failure in normal strength concrete (Mindess, Young, and Darwin, 2003).

Aggregates are typically thought to have minor effects on concrete compressive strength. In tensile strength and fracture properties, however, it holds more importance. In normal strength concrete, failures typically happen around an aggregate particle, not through, so the strength of the aggregate is not too important. If high-strength concrete is being used, the concrete paste is strengthened to the point that the aggregate particle is now the weak point in the system. In this case, aggregate strength will become the main component in concrete compressive strength. The shape, texture, and maximum aggregate size, on the other hand, typically play significant roles in normal strength concrete. Aggregate texture has a strong effect on the bond between aggregate and paste, thereby increasing the tensile strength capacity and the stress at which microcracking begins. While this alone would make for a stronger concrete, rough aggregates that would produce a stronger aggregate-paste bond also decrease workability. This creates a demand for more water in the mix, which usually offset the strength gains due to aggregate-paste bond improvements. Aggregate size can have an effect on both the compressive and tensile strength of the concrete. Large aggregates create larger stress concentrations when put under compressive loading and also can trap more bleed water, increasing porosity in the interfacial transition zone.

Large aggregates also tend to resist the volume changes that occur in the paste, which puts larger stresses on the paste fraction. These negative effects, however, are usually offset by increased workability (due to lower water demand) and therefore a lower w/cm that results in higher strength (Mindess, Young, and Darwin, 2003). The use of dense-graded aggregates may also have impact on concrete strength development through the potential increase in interparticle contact; however, the ultimate strength will still be a function of the w/cm and aggregate strength.

2.3.2 Maturity

Concrete strength development is a product of the hydration of cement particles in a concrete mixture. From the moment water comes into contact with cement, hydration reactions take place that will, over time, transform a fluid mixture into a hardened structure. The development of this strength is dependent on the concrete degree of hydration and temperature development. Maturity methods are used to compare the cement hydration progress made at different temperatures. The two most commonly used maturity methods are the Nurse-Saul method and the Equivalent Age method (Riding, 2007). The Nurse-Saul method generates a temperature-time factor that is defined as the integral of the temperature history and may be calculated as shown in Eq. 6. In the Nurse-Saul Method, *M(t)* is the maturity (°C-hrs) at time *t* (hrs), T_a is the average temperature (°C) during the time interval Δt (hrs), and T_o is the datum or baseline temperature used (°C).

$$M\ (t) = \sum (T_a - T_o) * \Delta t \qquad \text{Eq. 6}$$

Equation 7 shows the Equivalent Age Method for determining concrete maturity. Equivalent age maturity is defined as the age a concrete sample would have to be cured isothermally at some reference temperature T_r (°C) to have the same degree of reaction or properties as the sample cured at a different temperature. In this method, t_e is the equivalent age maturity (hrs), and Q is the activation energy divided by the gas constant (°K). One of the advantages of the equivalent age method is that it does a better job than the Nurse Saul method at predicting concrete strength level (Emborg, 1998; Mindess, Young, and Darwin 2003).

$$t_e = \sum\ e^{-Q\left(\frac{1}{T_a+273}-\frac{1}{T_r+273}\right)}\,\Delta t \qquad \text{Eq. 7}$$

2.3.3 Compressive strength

Once the maturity has been determined, models can then be used to predict the compressive strength development of the concrete mixture. While many models exist, two of the more common equations are given in Eq. 8 and 9 (Viviani, 2005).

$$f_c(t) = \ a + b * \log\left(\log\left(M(t)\right)\right), f_c \geq 0 \qquad \text{Eq. 8}$$

$$f_c(t_e) = \ f_{cult} * \exp\left(-\left(\frac{\tau_s}{t_e}\right)^{\beta_s}\right) \qquad \text{Eq. 9}$$

In these equations, f_c is the compressive strength development (MPa), a is a fit parameter which is usually negative (MPa), b is a fit parameter (MPa/°C/hr), f_{cult} is the ultimate

compressive strength parameter fit from the compressive strength tests (MPa), τ_s is a fit parameter (hrs), and β_s is a fit parameter. In ConcreteWorks, the program is set up to use Eq. 8 when the equivalent age maturity is used, and to use Eq. 9 when the Nurse-Saul maturity method is used. This helps prevent the occurrence of singular matrices when using these maturity methods to calculate elastic modulus (Riding 2007).

2.3.4 Elastic Modulus

Once compressive strength development has been generated, models can be used to predict the development of elastic modulus. This value is especially important in the context of bridge deck cracking, allowing the researcher to correlate the various volume change mechanisms that are occurring with the stresses that the changes generate. Essentially, as a concrete mixture develops a higher modulus of elasticity, volume changes generate higher stresses for each unit of movement. This relationship is shown in Eq. 10, where σ is the stress induced (psi), E is the elastic modulus of the concrete (psi), and ε is the strain in the concrete (in/in).

$$\sigma = E * \epsilon \qquad \text{Eq. 10}$$

While there are many models available for calculating the elastic modulus, most engineers and workers in the concrete industry are familiar with the ACI 318 (2008) calculation of elastic modulus:

$$\mathrm{E_c} = w_c^{1.5} * 33 * \sqrt{(f'_c)} \qquad \text{Eq. 11}$$

In Eq. 11, E_c is the elastic modulus of concrete, w_c is the unit weight of the concrete (lb/ft^3), and f'_c is the compressive strength of concrete (psi).

2.3.5 Tensile Strength

In the case of bridge deck cracking, proper modeling of concrete tensile strength is of great importance. Without a good model for tensile strength development, the engineer cannot determine whether or not the volume changes, and resulting stresses, occurring within a concrete system are significant enough to produce cracking. Raphael proposed one model for the development of tensile strength that is commonly used today (1984):

$$f_t = l * (f_c)^m \qquad \text{Eq. 12}$$

In Eq. 12, f_t is the tensile strength (MPa), f_c is the compressive strength of concrete (MPa), and l and m are fit parameters. In modeling bridge deck behavior, ConcreteWorks software will be used. In this application, splitting tensile strengths are used, and Raphael's fit parameters of 1.7 and 2/3 for l and m, respectively, are used for default fit parameter values (Raphael, 1984; Riding, 2007).

2.3.6 Creep and stress relaxation

Creep and relaxation play a key role in the development of stresses and potential for bridge deck cracking. Creep is a complicated mechanism, influenced by applied stresses,

water/cement ratio, curing conditions, temperature, moisture gradients, cement composition, chemical admixtures, aggregate properties, and specimen geometry (Mindess, Young, and Darwin, 2003). Though complicated, its effect on bridge deck cracking must be considered as relaxation due to creep can significantly reduce the stresses that are imposed on a bridge deck due to volume changes (thermal, autogenous, etc.). Figure 2.3 shows how the process of creep helps delay cracking through stress relaxation.

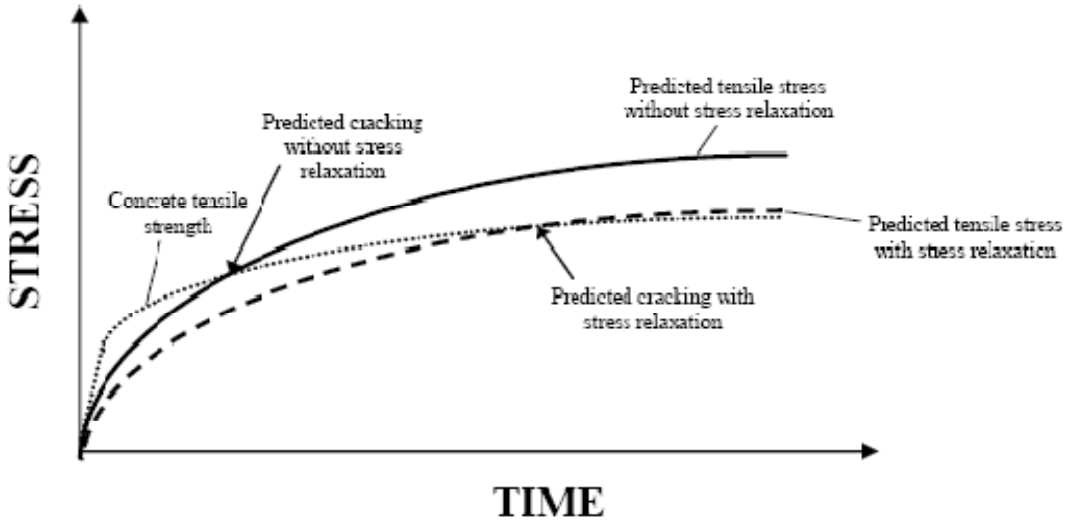

Figure 2.3: Time dependence of restrained shrinkage and creep (Mehta, 1993)

Many different models are available in the literature for evaluation of creep. ConcreteWorks presents a modeling structure for creep analysis that has been tailored for experimentation done using mixture designs and materials (both cement and aggregates) common to Texas construction projects. The program utilizes the Linear Logarithmic Model for calculating the early-age concrete stress relaxation. Equations are used to calculate the various slope components of the model, with adjustments for temperature modification, the aggregates used, and the Reitveld analysis of the cement used in the mixture. Further discussion, and the governing equations, of the Linear Logarithmic Model and the adjustments made in ConcreteWorks can be found in Riding (2007). One challenge remains in that early-age creep models (such as the one used in ConcreteWorks) must be linked to more traditional long-term creep models to address bridge deck cracking. This will be a key focus of the work proposed later in this report.

2.4 Bridge Deck Cracking

Bridge deck cracking is a complicated phenomenon that involves the interactions between volume changes, strength development, and the specific environment (restraint conditions) of the concrete system in use. Through the evaluation of many damaged bridge decks, researchers have been able to identify cracking patterns that are caused by the stresses generated within the concrete system, rather than those applied externally (through traffic and ground movement). Though cracking causes are numerous and interrelated, there are some methods for modeling bridge deck systems that attempt to predict whether a bridge deck will be susceptible to cracking during its lifespan. While most of these models only present a simplified

approach to the bridge deck cracking problem, usually taking into account one or two specific factors, they are a good place to start from in the attempt to make a model that takes into account all the mechanisms affecting a bridge deck system.

2.4.1 Mechanisms of Bridge Deck Cracking

As described in the introduction, bridge deck cracking has already been established as a serious concern for the nation's infrastructure. While initial deck cracking is not a failure of the bridge system, cracking allows the penetration of deleterious substances (air, water, chlorides, etc.) that can cause failure in bridge systems. Prediction and prevention of future bridge deck cracking issues can only be accomplished though knowledge of the various mechanisms and factors that are associated with this phenomenon. Figure 2.4 shows many factors that affect cracking in bridge decks.

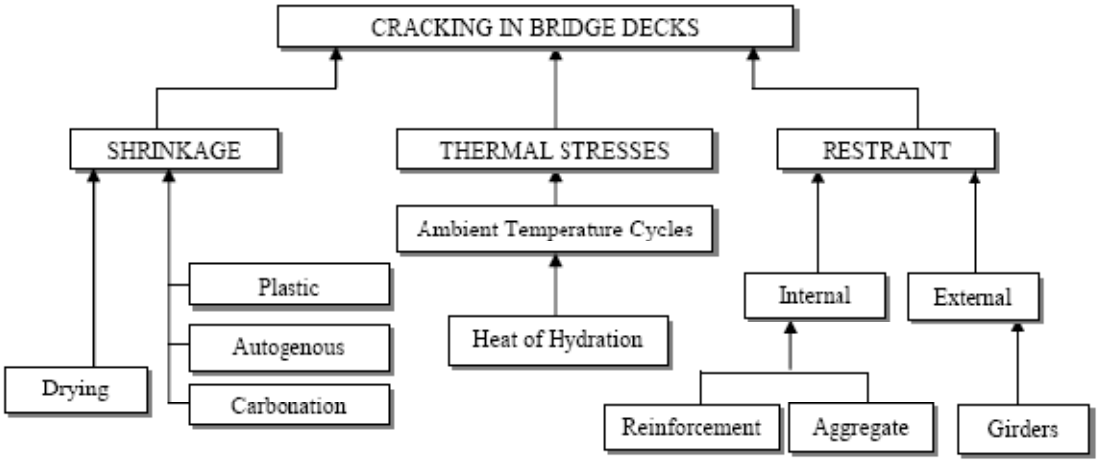

Figure 2.4: Causes of bridge deck cracking.

As can be seen in Figure 2.4, and as discussed in this review, volume changes account for much of the driving force in bridge deck cracking. However, all of the volume changes are innocuous until the concrete element is restrained. In bridge deck systems, restraint is typically generated from within the concrete, by aggregate and reinforcing steel, and externally, from the sub-base or superstructure of a bridge, including precast panels. If strains vary through the section, as they do with moisture and temperature gradients, then the member itself may even be considered a restraint to its own internal forces. Figure 2.5 shows a typical bridge deck support structure for Texas highways.

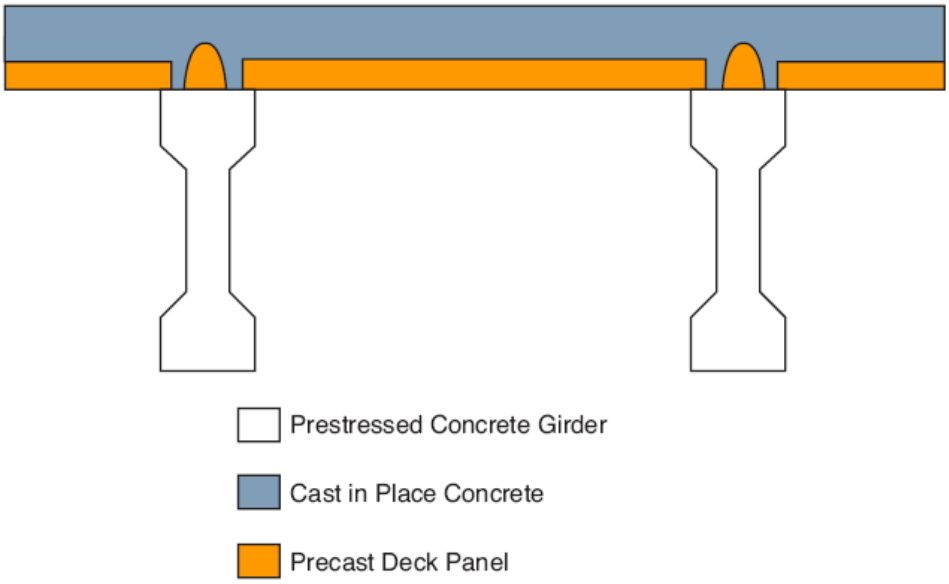

Figure 2.5: Typical precast, prestressed panel details.

2.4.2 Bridge Deck Cracking in Texas

Under TxDOT Project 4098, researchers evaluated several bridge decks in Texas that exhibited significant cracking. One of the structures that the researchers examined had developed a series of stair step crack patterns. These cracks were located on a deck running alongside a bridge expansion joint, on both sides of the joint. The stair step cracks intersected with pairs of longitudinal cracks that were spaced about 8-10 in. apart, and ran for about 25 ft. The transverse cracks were no longer than 4 ft long, Figure 2.6 shows the stair step cracking pattern that was common along the expansion joints of the Louetta Road Overpass. It should be noted that this deck was part of a FHWA project aimed at HPC and within this study, it was shown clearly that high-strength bridge decks are more prone to early-age cracking.

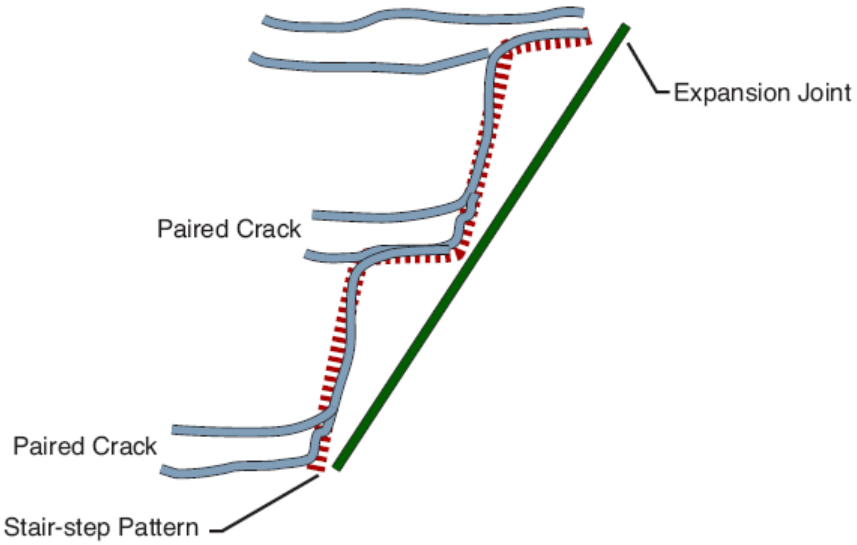

Figure 2.6: Typical stair step cracking.

The Dow Barge Canal Bridge in Freeport, Texas showed a different cracking pattern. Similar to the Louetta Bridge, the Dow Bridge had pairs of longitudinal cracks that ran along the spans. On the Dow Bridge, however, these longitudinal cracks carried much further than the Louetta Bridge, sometimes extending the length of the slab. The stair step pattern that was seen at the Louetta Bridge was also seen at the expansion joints of the Dow Bridge. One aspect that was different in the Dow Bridge was the occurrence of transverse cracks that spanned the length between longitudinal cracks, with about 8 ft. separating one transverse crack from another. The cracking pattern found in the Dow Barge Canal Bridge can be seen in Figure 2.7.

Researchers under TxDOT 4098 did identify the precast-prestressed panels as a trigger for cracking, generally due to the restraint that the panels provide against volume changes and due to the fact that the precast panels have already undergone most of their shrinkage (and creep), and the cast-in-place deck still has its entire shrinkage to undergo. In addition to the differential shrinkage issues, the Dow Barge Bridge also had issues with discontinuities at the butt joints. The precast panels, which are not connected along the longitudinal direction, would have small offsets in their height. When CIP concrete was laid continuously over these panels, cracks tended to form at the 8 ft. interval over which the butt joints were located, due to the increase in restraint.

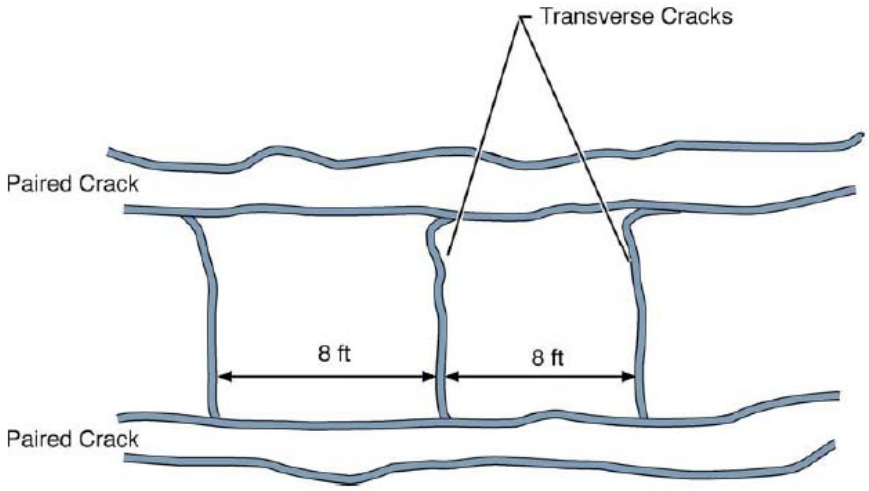

Figure 2.7: Typical transverse cracking.

Although there were significant cases of bridge deck cracking in Texas evaluated under TxDOT 4392, as depicted in Figures 2.6 and 2.7, it should be noted that the state of Texas does not have anywhere near as bad a problem as other states. Fortunately, TxDOT has known for quite a few years that moderate w/cm bridge decks are better than low w/cm mixtures that tend to exhibit more heat generation, more shrinkage, and less beneficial creep. Regardless, any improvements that can be made to the crack resistance of bridge decks will help to prolong the service life of our bridges.

2.4.3 Prediction and Modeling

While just understanding the mechanisms and factors that cause shrinkage in early-age concrete is a significant scientific achievement, it is the development of prediction and modeling systems that make this knowledge valuable to the engineering community. Unfortunately, such a tool does not exist today, at least not in a version that is user-friendly and aimed at TxDOT personnel and contractors. To develop such a tool or in this case, a module to be integrated into ConcreteWorks, several technical issues must be addressed, as highlighted below:

Modeling of creep and stress relaxation, bridging the gap between early-age creep models refined and applied under TxDOT 4563 and more classical long-term creep models.

- Understanding of how moisture loss leads to gradients in moisture (and shrinkage) and how this can ultimately be modeled.
- Evaluation of how the various volume changes, individually or in combination, result in stress and potential cracking.

Chapter 3. Work Plan

The remainder of this report describes the work plan to be carried out for the remainder of this project, with both laboratory and field components included in the study. The materials and mixture portions are described first, followed by a summary of the laboratory and field evaluations to be performed. Lastly, the framework for how the computational and modeling aspects will be addressed in this bridge deck cracking module is presented.

3.1 Materials and Mixture Proportions

A wide range of materials will be evaluated in this project in a comprehensive laboratory-based research program. The materials, shown in Table 3.1, have been selected based on the research team's past experience with TxDOT bridge deck construction and with research projects (TxDOT Projects 4563, 4098, etc.) that focused on deck-related issues, such as heat of hydration and shrinkage cracking. All the materials listed above will not be included in all facets of this project. The materials will be selected based on prioritization of research objectives and relevancy of specific materials to specific testing regimes. For example, small dosages of polypropylene fibers (i.e., 1 to 1.5 pcy) will only be included in studies focusing on plastic shrinkage cracking, which represents the major application for such low dosages of fibers.

Table 3.1: Materials to be included in laboratory evaluations

Materials	Number of Sources or Types	Details
Portland cement	2	• Type I (high-alkali) • Type I/II (low-alkali)
Fly ash	5	• Low-CaO (<5 percent) • Moderate-CaO (10-20 percent) • High-CaO (20-25 percent) • Very high-CaO (25-30 percent) • Ultra-fine fly (moderate-CaO) – [UFFA}
Silica Fume	1	• Densified
GGBF Slag	1	• Grade 120
Coarse aggregate	2	• Siliceous river gravel • Crushed limestone
Fine aggregate	1	• Siliceous river sand
Chemical admixtures	2	• Normal water reducer • Shrinkage-reducing admixture
Fiber reinforcement	2	• Monofilament polypropylene ("microfiber" for plastic shrinkage control) • Monofilament synthetic ("macrofiber" for structural enhancement)

The mixture proportions to be used in this project will be based primarily on Texas DOT Class S concrete, which is typically used for bridge deck construction. A typical Class S mixture is a 6-sack mixture (564 pcy of cement) with a maximum w/cm of 0.45. Most mixtures will be

cast with this general composition, and when SCMs are used, they will be used as a mass replacement for cement. For selected mixtures, the impact of paste content on key shrinkage mechanisms will be evaluated. One method of reducing paste content is to optimize aggregate gradation—this approach will also be explored for selected mixtures. The team will consider several methods of optimizing aggregate gradation, including the Shilstone method, 18/8, and 0.45 power curve. The specific mixtures to be evaluated are described later in this report as they relate to the specific testing regimes (e.g., cracking frame).

3.2 Laboratory Evaluations

3.2.1 Cracking Frames

The most important component of the laboratory testing program, and for this project for that matter, is the innovative use of the rigid cracking frame and free shrinkage set-up that was the main driver behind TxDOT 4563. This set-up will be used to test the behavior of various bridge deck materials and mixture proportions when exposed to typical TxDOT field conditions. It should be noted that for practical and technical reasons, the role of plastic and drying shrinkage will not be evaluated using the rigid cracking frames, and as such, the main goal of the cracking frame tests are to evaluate the effects of thermal and autogenous deformations on stress development in bridge deck mixtures. As described later, information will be obtained later, in the form of pre-existing databases, predictive equations, or models that will allow the team to incorporate the effects of plastic and drying shrinkage, as well as creep and relaxation.

Before describing the mixtures to be evaluated, a brief description of the cracking frame approach is presented. Figure 3.1 shows a drawing of the rigid cracking frame and Figure 3.2 shows a picture of the test setup (Riding 2007). A 6” x 6” x 49” (150 x 150 x 1250 mm) concrete specimen is placed, consolidated, and cured in the rigid cracking frame. The formwork of the rigid cracking frame allows the temperature of the freshly placed concrete to be conditioned to simulate various structural elements. The temperature of the rigid cracking frame specimen is controlled using a programmable refrigerating/heating circulator that circulates a 50/50 mixture of water and ethylene glycol through copper pipes in the formwork and cracking frame crossheads. The main purpose of the crossheads is to grip the concrete so that the rigid Invar side bars restrain the concrete specimen against deformation (Whigham 2005).

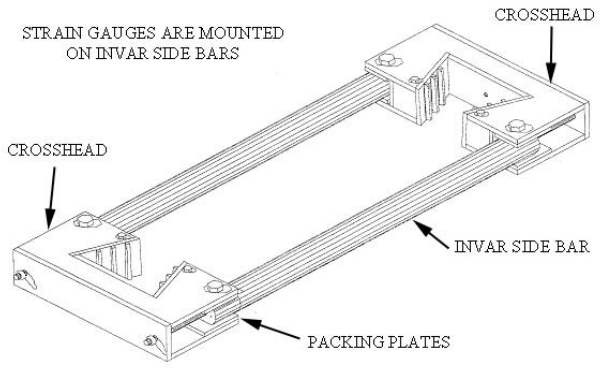

Figure 3.1: Rigid Cracking Frame Drawing (Riding 2007)

Figure 3.2: Photograph of Rigid Cracking Frame (Whigham 2005)

The stress in the rigid cracking frame is monitored with strain gauges mounted on the 3.94" (100 mm) diameter Invar restraining bars. These bars are designed to provide a high level of restraint while allowing small deformations that are measured with strain gauges (Whigham 2005). The restraining bars hold the crossheads 44" (1250 mm) apart. Invar has a very low coefficient of thermal expansion compared to mild steel. Invar is thus used for the bars to minimize thermal effects on the length change of the restraining bars. Although minimal (or negligible in some cases), the thermal movement of the Invar restraining bars is subtracted from the measured strain to calculate the actual stress induced strain in the Invar bars.

A free shrinkage frame has been developed to measure the free thermal and autogenous dilation of the concrete mixture (Riding 2007). Figure 3.3 shows a diagram and picture of the free shrinkage frame. The free shrinkage specimen dimensions are 6" x 6" x 20.4" (150 x 150 x 520 mm). The bottom bar is made of Invar, as are the two threaded rods that are embedded in the concrete. The threaded rods are screwed onto linear potentiometers, which are then threaded onto 1" x 1" (25 x 25 mm) plates which are embedded in the concrete. Layers of plastic are used between the concrete and the formwork, with a lubricant applied under each layer, to reduce friction between the specimen and the formwork. The copper pipes in the free shrinkage frame's formwork are connected in series with the cracking frame and circulator to ensure that the free shrinkage frame's temperature stays within about 1.8° F (1° C) of the temperature of the concrete in the rigid cracking frame. The temperature is recorded using two thermocouples. The free shrinkage is initialized and set to zero at initial setting as determined following ASTM C 403 (2006). The samples for the setting test are also match-cured to the temperature history of the free shrinkage frame, as are other samples (4" x 8" cylinders) that are tested for mechanical behavior (compressive strength, elastic modulus) at various early ages.

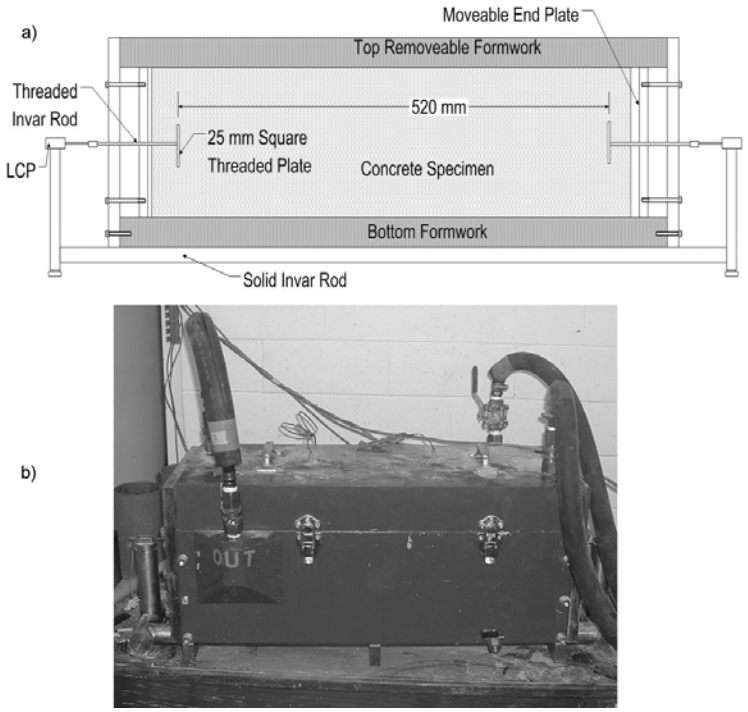

Figure 3.3: Free Shrinkage Frame a) Diagram and b) Photograph

The overall cracking frame approach (including free shrinkage frame and parallel mechanical property testing) is very powerful in that it can allow for any simulated time-temperature history that may be encountered in the field. For this project, the team will take a similar approach to how thermal cracking was evaluated and ultimately modeled and incorporated into ConcreteWorks. All the frames and specimens can be subjected to isothermal testing (to isolate autogenous deformations) or they can be tested using time-temperature history that simulates that of an actual bridge deck placement. This can be accomplished by conducting a semi-adiabatic or Q-drum test to determine the relevant hydration parameters, and these parameters are then used as inputs to a ConcreteWorks-based simulation to determine the thermal distributions throughout a hydrating bridge deck that is subjected to specific exposure conditions (e.g., ambient temperature, humidity, windspeed, etc.).

Figure 3.4 illustrates this overall approach to testing using this integrated testing regime. The approach outlined in Figure 3.4 was used throughout TxDOT 4563 and the data served as the basis for the development of the mass concrete cracking model. Over the past couple of years, a similar approach has been followed for evaluating the impact of fly ash (type and dosage) on bridge deck cracking, under a TxDOT interagency contract (IAC). Table 3.2 summarizes the completed testing matrix, which involved a total of 12 concrete mixtures subjected to simulated hot weather concreting conditions, with a delivered concrete temperature of 90 °F. For these mixtures, semi-adiabatic calorimetry was performed to generate the relevant hydration parameters (α, β, τ) and ConcreteWorks (using the calculated activation energy from ConcreteWorks based on the materials/mixture proportions) was then used to simulate the time-temperature history for a bridge deck, with a delivered concrete temperature of 90 °F and simulated mid-summer ambient conditions (based on 30-year climatic data integrated into ConcreteWorks). Parallel free shrinkage prisms (following ASTM C 157) were also cast, moist

cured for different curing periods (8-10 days), and then subjected to drying conditions. This was aimed at directly quantifying the effect of bridge deck wet curing on drying shrinkage behavior.

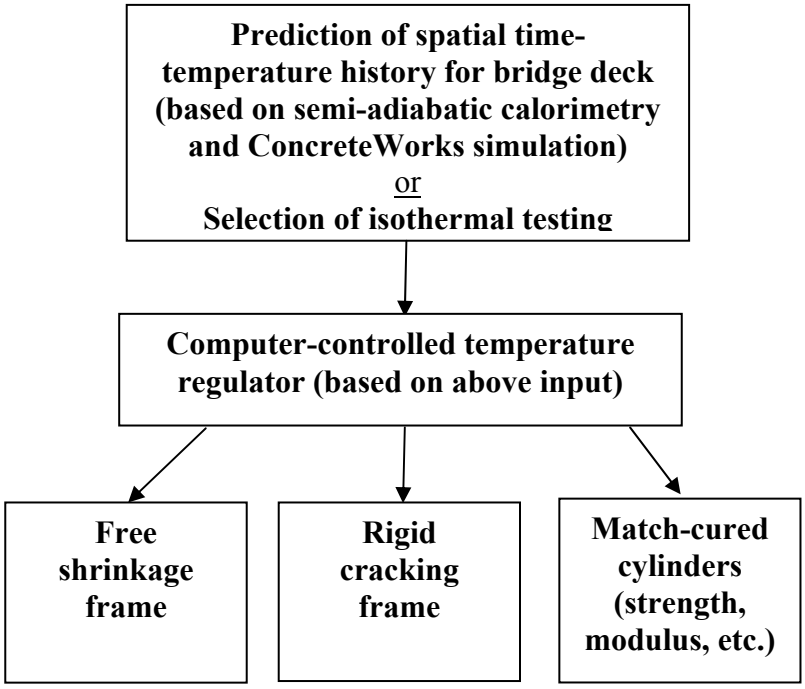

Figure 3.4: Conceptual approach to overall cracking frame test set-up

Table 3.2: Completed Testing Matrix for IAC on Impact of Fly Ash on Shrinkage Cracking

Mixture*	Cement	Dose
Control 1	Type I/II (low alkali**)	0%
Fly Ash 1 (CaO = 2-5 percent)	Type I/II (low alkali)	25%
Fly Ash 2 (CaO = 12-17 percent)	Type I/II (low alkali)	25%, 35%
Fly Ash 3 (CaO = 20-24 percent)	Type I/II (low alkali)	25%, 35%
Fly Ash 4 (CaO = 25-30 percent)	Type I/II (low alkali)	25%, 35%
Fly Ash 4 and UFFA	Type I/II (low alkali)	35% FA + 10% UFFA
Control 2	Type I/II (high alkali***)	0%
Fly Ash 1 (CaO = 2-5 percent)	Type I/II (high alkali)	25%
Fly Ash 4 (CaO = 25-30 percent)	Type I/II (high alkali)	25%

* High Temperature = summer pour (90 °F placement temperature)
** Low-alkali = 0.4-0.6 percent Na_2O_e
*** High-alkali = 0.8-1.0 percent Na_2O_e

The results of the IAC study are highlighted in Table 3.3. Typical results of free shrinkage frame and rigid cracking frame tests are shown in Figures 3.5 and 3.6, respectively, for the control, low-alkali cement mixture. A more detailed analysis of these test results will be performed under this current project after the additional 32 mixtures are tested, as described next. This combined dataset will be extensive, with a total of 44 tests to be conducted. Once the tests have been conducted across a range of materials, mixture proportions, and simulated environmental conditions, the research team will develop predictive models for creep, stress development, and mechanical strength development—these overall results will then be used to develop the thermal cracking prediction model for this project, using a similar approach that was used under TxDOT Project 4563 for mass concrete elements.

Table 3.3: Summary of Cracking Frame Results for IAC Study

Mixture Designation	Portland Cement	Fly Ash	Fly Ash Dosage (%)	Maximum Temperature (˚F)	Temperature at Failure (˚F)	Stress at Failure (psi)	Stress / Strength at Failure
C1L	Type I/II (low-alkali)	None	0%	113.9	67.7	353.0	0.490
FA1L-25	Type I/II (low-alkali)	FA1	25%	102.8	76.6	152.1	0.264
FA2L-25	Type I/II (low-alkali)	FA2	25%	100.2	76.5	185.5	0.314
FA2L-35	Type I/II (low-alkali)	FA2	35%	100.3	71.2	213.6	0.386
FA3L-25	Type I/II (low-alkali)	FA3	25%	102.7	62.5	340.5	0.528
FA3L-35	Type I/II (low-alkali)	FA3	35%	97.9	69.5	314.7	0.535
FA4L-25	Type I/II (low-alkali)	FA4	25%	102.6	76.9	222.4	0.343
FA4L-35	Type I/II (low-alkali)	FA-4	35%	100.0	77.5	233.2	0.418
FAPL-25	Type I/II (low-alkali)	FA-4*	25%	104.1	60.0	303.4	0.530
FA4L-35U	Type I/II (low-alkali)	FA-4 and Micron3	35% FA + 10% UFFA	114.6	80.7	338.4	0.610
C2H	Type I/II (high-alkali)	None	0%	104.3	64.7	348.5	0.566
FA1H-25	Type I/II (high-alkali)	FA1	25%	114.7	69.9	288.8	0.650
FA4H-25	Type I/II (high-alkali)	FA-4*	25%	116.2	68.1	304.1	0.548

Note: FA-4* was used on selected mixtures instead of FA-4 due to shortages of FA-4.

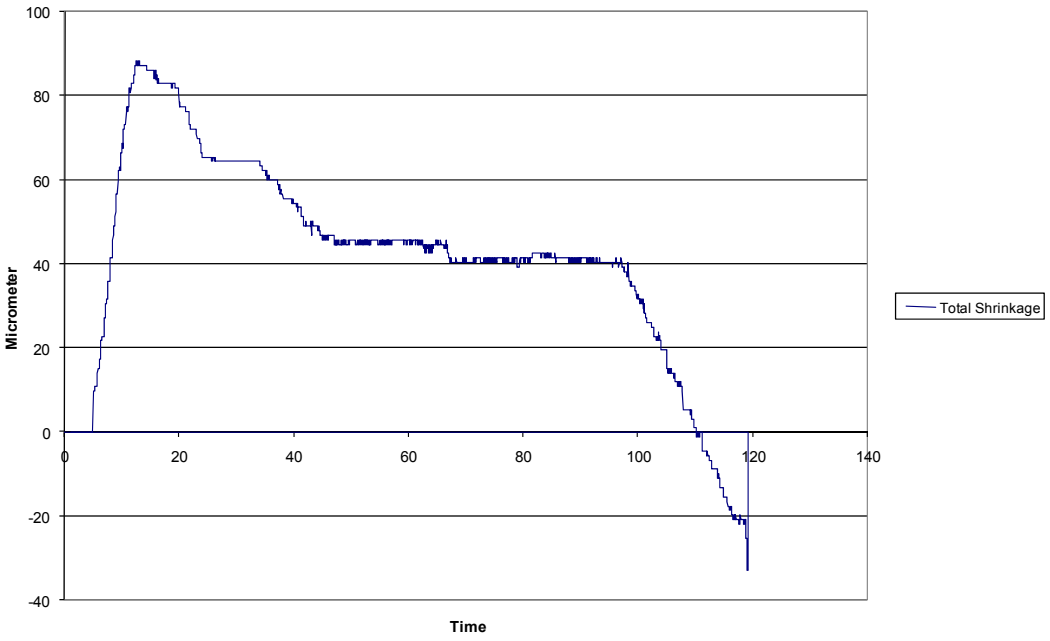

Figure 3.5: Typical free shrinkage frame results (for mixture C1L)

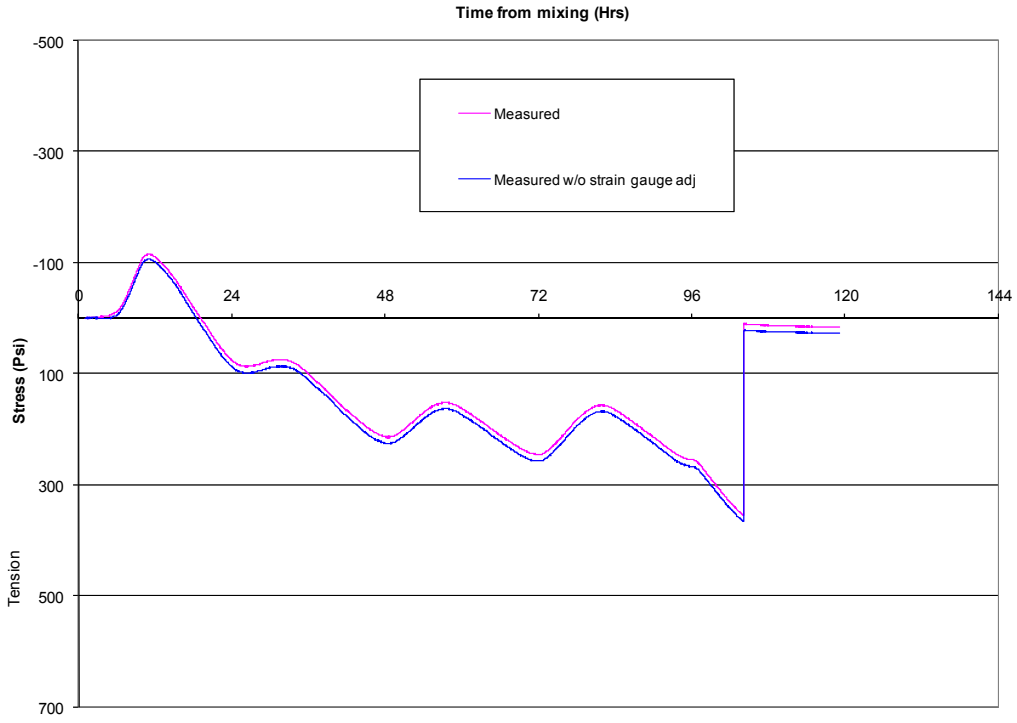

Figure 3.6: Typical rigid cracking frame results (for mixture C1L)

A similar approach to the IAC project summarized in Table 3.2 will be taken for the 32 cracking frame tests to be conducted over the course of the next two years, with a combination of realistic time-temperature histories and isothermal testing. The research team will integrate all the data generated under this IAC into the dataset for this proposed research, thereby making

direct use of the synergy between the two projects and benefiting from the augmented database of test data. For convenience, the same designations for fly ash CaO content shown in Table 3.2 will be used in this report (Fly Ash 1, Fly Ash 2, etc.) as the same four fly ashes will be included in the current study. Table 3.4 summarizes the 32 cracking frame tests that will be conducted as part of this project. The research team is confident the data generated between the 32 tests from this project and the 12 tests from the IAC will allow the team to model key aspects of early-age bridge deck performance. The two control mixtures will be repeated under the "H" or hot weather concreting temperature regime to tie the results of these tests to the IAC work.

Table 3.4: Cracking Frame Testing Matrix for This Project

Mixture description	Cement alkalies*: High (H) or Low (L)	Coarse Aggregate Type: Siliceous river gravel (SRG) or Limestone (LS)	SCM Dosage (% mass replacement of cement)	Cracking Frame Testing Regime**		
				H	C	I
Control *(low-alkali cement)*	L	SRG	-	x	x	x
Control *(high-alkali cement)*	H	SRG	-	x	x	
Control *(low-alkali cement)*	L	LS	-	x	x	
Fly ash 1	L	SRG	25% Fly Ash 1		x	
Fly ash 1	H	SRG	25% Fly Ash 1		x	
Fly ash 2	L	SRG	25% Fly Ash 2		x	
Fly ash 2	L	SRG	35% Fly Ash 2		x	
Fly ash 2	H	SRG	25% Fly Ash 2	x	x	
Fly ash 3	L	SRG	35% Fly Ash 3		x	
Fly ash 3	L	LS	35% Fly Ash 3	x	x	
Fly ash 4	L	SRG	35% Fly Ash 4		x	
Fly ash 4	H	SRG	35% Fly Ash 4	x	x	
Ternary blend (Fly Ash 4 with UFFA)	L	SRG	35% Fly Ash 4 + 10% UFFA		x	
GGBF slag	L	SRG	35% Slag	x	x	
GGBF slag	L	SRG	50% Slag	x	x	
GGBF slag	H	SRG	50% Slag	x	x	
GGBF slag	L	LS	50% Slag	x	x	
Shrinkage-reducing admixture	L	SRG	-	x	x	x
Optimized gradation (allowing for reduced paste content)	L	SRG	-	x		

* Low-alkali = 0.4-0.6 percent Na_2O_e, High-alkali = 0.8-1.0 percent Na_2O_e

** H=Hot weather pour; C=cold weather pour; I=Isothermal (fixed temperature) conditions

For selected mixtures, internal relative humidity sensors and strain gages will be imbedded in the free shrinkage specimens and potentially the rigid cracking frame specimens, allowing for the simultaneous measurement of internal humidity, which can be correlated with autogenous deformations. This unique approach will allow for the potential development of an autogenous shrinkage model that directly links self-desiccation and microstructural development with actual strain and restrained stress development across a range of typical materials and mixture proportions. In addition, after the completion of the free shrinkage test, the instrumented specimens will be removed and moist-cured up to an age of 8-10 days (typical of bridge deck curing practice), then placed in the drying shrinkage room (73 F, 50% RH), and the relationship between internal relative humidity and drying shrinkage can be quantified. The long-term shrinkage data will then be compared to "off-the-shelf" shrinkage models, such as B3 or CEB 90. At the same time, the long-term drying shrinkage data can be correlated with internal relative humidities; and these results will prove quite valuable when considering moisture gradients, as described next. This data can then be compared and extrapolated to actual specimens subjected to uniaxial drying or to actual bridge decks instrumented with internal RH sensors and strain gages.

It is a goal of this project, albeit a lofty one, to develop a model to predict moisture gradients for a range of mixtures and subjected to various ambient conditions, and to use the predicted moisture gradients (or more accurately, gradients in internal relative humidity) to assess stresses due to drying shrinkage gradients. This may not be technically possible as it is a very complex issue that deserves much more attention than can be provided from this project alone—however, the team is confident that as a minimum, a first-order estimate can be made in predicting the effects of drying conditions on moisture gradients in concrete.

The remainder of this section describes how each of the key parameters will be addressed through laboratory and/or field evaluations or through the use of existing data, predictive equations, or models. Each of the key parameters are described separately below, but it should be noted that most of the sources of volume change occur simultaneously, and the model will, thus, evaluate the combined effects of the various sources of strain (and resultant strain, translated into stress based on degree of restraint, and adjusted based on creep and stress relaxation).

3.2.2 Plastic shrinkage

As described earlier, plastic shrinkage is a complex phenomenon, complicated by an initial battle between evaporation and bleeding; and the subsequent battle between tensile strength and stresses emanating from plastic shrinkage. The current method advocated by ACI and used by most agencies (including TxDOT) is to simply and solely estimate the evaporation rate, using Menzel's equation, and to mandate preventive measures when the calculated evaporation rate exceeds a threshold value, most commonly 0.2 $lb/ft^2/hr$. In addition to the inherent inaccuracies of using Menzel's equation, which was based on evaporation of water from a free surface, current practice does not account for either the bleeding rate or the rate of tensile strength development. A review of available literature will be performed to attempt to reconcile these shortcomings, and this evaluation of existing literature will serve as the basis for integrating plastic shrinkage cracking into the overall model developed under this project. It is not the intention to directly evaluated plastic shrinkage cracking as part of these efforts, but some evaluations of early-age tensile strength may be initiated to better quantify the very early-age tensile strength of concrete, especially for mixtures containing small amounts of synthetic fibers

or large amounts of structural, synthetic fibers as these materials have been used increasingly for bridge deck construction worldwide.

The current version of ConcreteWorks uses the modification to Menzel's equation that were proposed by Al-Fadhala and Hover (2001), but this modification is based on a somewhat limited database—more research is needed to develop a more robust approach to estimating evaporation rates. For the field evaluations described later in this report, data will be collected on evaporation and bleeding rates for comparison to the evaporation rates predicted by Al-Fadhla and Hover (2001).

3.2.3 Autogenous shrinkage

Because the typical w/cm values used for TxDOT bridge decks (0.40 to 0.45) are above those for which autogenous shrinkage is a major concern, only limited emphasis will be placed on this issue. Through the cracking frame testing, significant data will be generated on the autogenous deformations of typical deck mixtures, and this data will be coupled with data generated in the past year or so at UT-Austin by this same research team on mixtures will lower w/cm ratios, and this breadth of data should provide a strong basis for estimating autogenous deformations.

ConcreteWorks currently uses a modified version of the autogenous shrinkage model developed by Hedlund (2000). Hedlund developed and published a model based on his dataset for autogenous shrinkage starting at 24 equivalent age hours. The model is based on an ultimate autogenous shrinkage calculated from the w/cm that is altered to account for temperature effects. Equations 13-16 show the model proposed by Hedlund for calculating the autogenous shrinkage with the concrete equivalent age:

$$\varepsilon_{SH} = \varepsilon_{su} \cdot \beta_{s0}(t_e) \cdot \beta_{ST}(T) \quad \text{Eq. 13}$$

$$\varepsilon_{su} = (-0.65 + 1.3 \cdot \frac{w}{cm}) \cdot 10^{-3} \quad \text{Eq. 14}$$

$$\beta_{s0}(t_e) = \exp\left(-\left[\frac{t_{s1}}{t - t_{s0}} \right]^{\eta_{SH}} \right) \quad \text{Eq. 15}$$

$$\beta_{ST}(T) = a_0 + a_1 \cdot \left[1 - \exp\left(-\left(\frac{T}{T_1} \right)^{b_1} \right) \right] + a_2 \cdot \left[1 - \exp\left(-\left(\frac{T}{T_2} \right)^{b_2} \right) \right] \quad \text{Eq. 16}$$

where t_{s0} (days), t_{s1} (days), η_{SH}, a_0, $a1$, $a2$, $b1$, $b2$, $T1$ (°C), and $T2$ (°C) are fit parameters.

Hedlund recommends setting the parameters ts1, ηSH, a0, a1, b1, b2, T1 (°C), and T2 (°C) may be set equal to 5 days, 0.3, 0.4, 0.6, 9 °C, 2.9, 55 °C, and 7, respectively. Additionally, he recommends setting the parameter a2 equal to 1.3 for normal strength concrete and 0.1 for high performance concrete. The parameter ts0 is the time at which the concrete shrinkage begins. Before this time, the concrete autogenous shrinkage is set equal to zero (Hedlund, 2000).

The autogenous shrinkage model used in ConcreteWorks modifies the model developed by Hedlund to reduce the w/cm at which autogenous shrinkage develops, the time at which autogenous shrinkage begins, and does not include the temperature modification term. The ultimate concrete shrinkage value used in ConcreteWorks is calculated using Equation 17:

$$\varepsilon_{ault} = \left(-0.94 + 2.238 \cdot w/cm\right) \cdot 10^{-3} \qquad \text{Eq. 17}$$

The w/cm at which autogenous shrinkage develops in ConcreteWorks is 0.42, which corresponds to the theoretical w/cm at which complete hydration is possible (Mindess, Young, and Darwin, 2003). Additionally, autogenous shrinkage begins at the virtual time-of-set, not at 24 equivalent age hours as in the Hedlund model.

As previously mentioned in this report, selected concrete specimens to be tested using the "free shrinkage frame" will be instrumented with internal humidity sensors and strain gauges, and when testing is performed under isothermal conditions, a correlation between internal relative humidity and autogenous shrinkage will be developed. These same, instrumented specimens will then be subjected to drying conditions (as described in the next section), and the internal relative humidity data will be used to link drying shrinkage strains to internal changes in moisture conditions. The information/data generated via the use of internal relative sensors will be very useful in that under isothermal conditions, a relationship between drying caused by self-desiccation can be attained, and subsequent analyses of pore size distribution using mercury intrusion porosimetry (MIP), coupled with the measurement of degree of hydration (by non-evaporable water content determination), can yield very useful information between the emergence of microstructure and pore size distribution, internal relative humidity, and autogenous shrinkage.

Lastly, the research team will attempt to address one potential shortcoming of the modified Hedlund model. That is, autogenous shrinkage is currently predicted using the maturity concept, which involves determining the time required for the cement paste to achieve the same level of development, at a certain temperature, as that under the effect of the actual time-temperature history (Turcry et al. 2002). However, actual autogenous shrinkage has proven to be dependent on temperature as well. Further research into this topic will be initiated under this project by performing isothermal testing on free shrinkage specimens at different temperatures, with the intention of elucidating and quantifying the temperature dependence of autogenous shrinkage.

3.2.4 Drying shrinkage

The drying shrinkage of concrete bridge decks can lead to significant cracking. Fortunately, in the state of Texas, past experience has led to bridge decks that are generally not as susceptible to drying shrinkage as other states. Specifically, TxDOT specifies a maximum w/cm of 0.45 and most decks are cast in the range of 0.40 to 0.45. TxDOT has learned that casting high-strength (or some would say HPC) bridge decks tends to result in early-age cracking, fueled by thermal, autogenous, and drying shrinkage and exacerbated by the fact that such mixtures exhibit high elastic modulus and low creep. These types of decks have been referred to as "HPC between the cracks" by various practitioners. Direct evidence of this was documented by Folliard et al. (2003) for the experimental HPC bridge deck cast for the Louetta Bridge. This deck did not represent current practice at the time but was constructed as part of a FHWA-funded project on HPC, but the experience gained from this structure has reinforced TxDOT's goal of producing more ductile bridge decks and avoiding early-age cracking. In addition, TxDOT has specified wet-mat curing of bridge decks, typically from 8 to 10 days, and this has resulted in more durable and crack-resistant bridge decks. Although drying shrinkage of

bridge decks may not be as significant of a factor as it is in other states, it clearly needs to be addressed and included in the model that is developed under this project.

As stated previously, drying shrinkage was not considered in the mass concrete cracking model developed under TxDOT 4563 as drying shrinkage of such large elements (with large volume/surface ratios) is far outweighed by autogenous and thermal stresses. However, for bridge decks, drying shrinkage must be considered. Furthermore, not only must the overall drying shrinkage of the deck be considered, but the moisture gradient that emerges after wet curing is ceased should be addressed.

As stated previously, there have been a wide range of studies that have measured the drying shrinkage and/or creep of concrete. The large database generated under these studies has led to the development of various predictive models (B3, CEB 90, etc) for drying shrinkage and creep. The research team will evaluate both the B3 or CEB 90 models as they appear to be favored by practitioners and researchers. It should be noted that it will not be the intention of this project to generate thousands of data points on drying shrinkage as this would be duplicative of the numerous studies performed to date. To illustrate the point that a great amount of data already exist on drying shrinkage, Al-Manaseer and Lam (2005) reported that the RILEM Data Bank consists of 7053 shrinkage data points (426 shrinkage data sets) and 8790 creep data points (518 data sets). As such, the intention of the research conducted under this project will be to generate a set of data representative of Texas materials to determine which model predicts long-term drying shrinkage the best, and then to incorporate this model (or modification thereof) into the bridge deck cracking model. The drying shrinkage model(s) selected for the bridge deck cracking model will benefit from the extensive database of climatic data (e.g., temperature, relative humidity, windspeed, etc.) stored within ConcreteWorks, which are parameters used to define the degree of drying to be experienced in a given locale. In addition, the maturity function that is already integrated into ConcreteWorks for bridge decks will allow for calculation of compressive strengths throughout the deck, and these values, as well as values of elastic modulus that can be estimated based on these strength values, will serve as other requisite inputs to long-term drying shrinkage (and creep) models.

As already mentioned in this report, selected concrete specimens to be tested using the "free shrinkage frame" will be instrumented with internal humidity sensors and strain gauges, and when testing is performed under isothermal conditions, a correlation between internal relative humidity and autogenous shrinkage will be developed. Upon completion of the free shrinkage portion of the test, these specimens will then be subjected to drying conditions (73 ºF, 50% RH), and these data will then be compared to "off-the-shelf" shrinkage models, such as B3 or CEB 90. At the same time, the long-term drying shrinkage data can be correlated with internal relative humidities, and these results will prove quite valuable when considering moisture gradients, as described next.

In order to predict and model moisture gradients and related volume changes in bridge decks, significant data will be needed to be generated. For selected concrete mixtures, concrete prisms will be stored long-term at 73 ºF at selected relative humidities (using "shrinkage room" or specimens stored above saturated salt solutions to maintain a target relative humidity). RH sensors will be imbedded in the concrete specimens. Because the specimens will be relatively small (3" x 3" in cross section), the specimens will ultimately reach equilibrium with the environment in which they are placed; thus, a correlation will be made between equilibrium relative humidity and total shrinkage strain. This data can then be compared and extrapolated to actual specimens subjected to uniaxial drying or to actual bridge decks instrumented with

internal RH sensors and strain gages. It is expected that a model will be developed under this project that can predict moisture gradients for a range of mixtures and subjected to various ambient conditions, and that these predicted moisture gradients (or more accurately, gradients in internal relative humidity) can be used to estimate stresses due to drying shrinkage gradients.

3.2.5 Thermal effects

A heat of hydration model was developed under TxDOT 4563 and was coupled with a heat transfer model specifically for bridge decks—this capability is built into the latest version of ConcreteWorks (V. 2.0.6). However, because the main thrust of TxDOT 4563 was more focused on mass concrete, only limited field calibration and validation were performed on bridge decks. It is proposed that the starting framework for the heat generation module of the bridge deck cracking model be the same as the one developed under TxDOT 4563 as there were significant calorimetry data generated under that project on mixtures similar in composition and proportions to bridge deck mixtures. A wide range of mixtures with w/cm between 0.40 and 0.45 were cast and tested, including mixtures with a wide range of chemical admixtures and SCMs. Some additional testing, described in Phase II, will be initiated under this project involving isothermal and particularly semi-adiabatic calorimetry as semi-adiabatic calorimetry or "Q-drum" testing is routinely performed the week before cracking frame tests to ensure that accurate hydration parameters are used to generate realistic time-temperature histories for the cracking frame testing regime.

The heat transfer model that will serve as a starting point for the bridge deck cracking module will take into account the various factors shown in Figure 3.7. Additional details on these various factors can be found in Riding (2007).

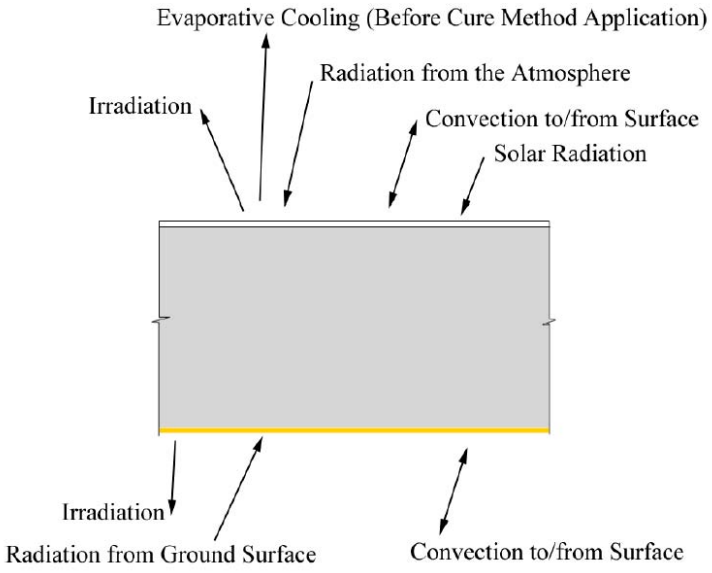

Figure 3.7: Summary of boundary conditions affecting heat transfer to/from bridge deck

As stated previously, more work is needed under this project to calibrate and validate the heat of hydration/heat transfer model for bridge decks. Only one bridge deck was instrumented under TxDOT 4563, shown in Figure 3.8. This bridge was part of a full-scale structural evaluation performed at Ferguson Structural Engineering Laboratory. The deck was heavily

instrumented to measure temperatures throughout the deck and both above and between steel girders. Note that the deck was cast directly on steel pans as this was the focus of the structural evaluation—however, most bridge decks in Texas are cast onto precast concrete panels. Figure 3.9 shows the temperatures developed above and between the girders in the instrumented bridge deck. The temperature in the bridge deck was much higher above the girders than between them, because the girder trapped in heat that otherwise would have been lost due to convection under the deck. Figure 3.10 shows the temperature development through the deck cross-section between the girders. The top temperature is shown as Sensor 3, the middle as Sensor 2, and the bottom as Sensor 1. The difference in temperature in the vertical direction was limited to less than 8°C (14°F), mainly because of the insulation provided by the curing blanket on the deck. The bottom of the deck tended to be cooler than the top of the deck because of the lack of insulation underneath the deck, and the solar radiation component that influences the top more than the bottom.

Figure 3.8: Photograph of instrumented bridge prior to deck placement

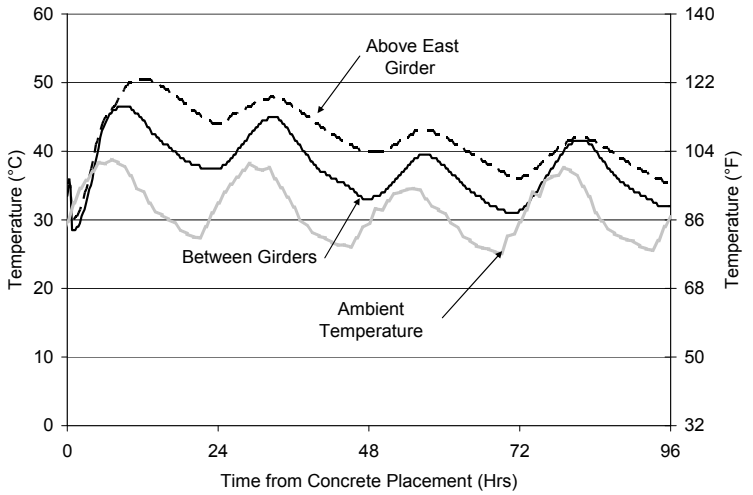

Figure 3.9: Temperature development in bridge deck at mid-depth, above, and between girders (Riding et al. 2009)

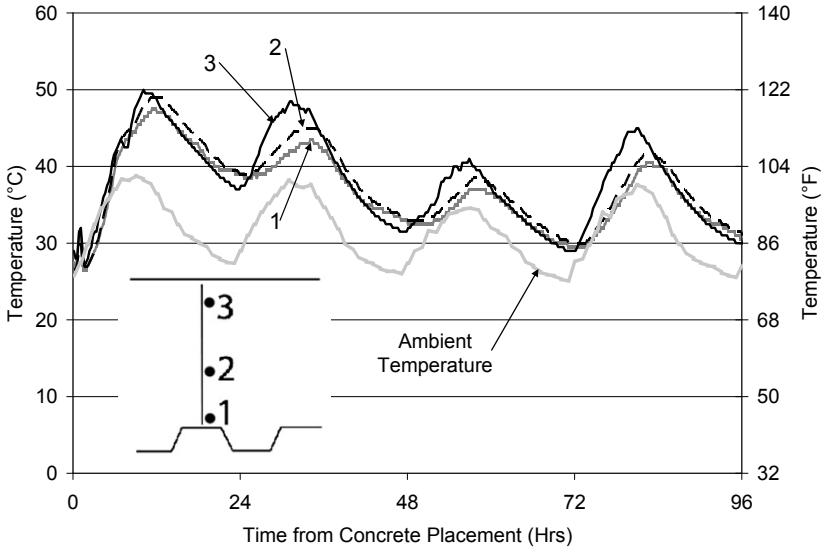

Figure 3.10: Vertical temperature profile in the bridge deck between girders (Riding et al. 2009)

The temperature profiles shown in Figures 3.9 and 3.10 are important in that they illustrate the importance of boundary conditions in bridge decks, especially the impact of girders on thermal profiles. Of course, the results would have been considerably different if the deck were cast over precast panels and precast concrete girders, due to the difference in thermal mass and thermal conductivity. More field tests are essential to properly calibrate and validate the thermal model developed under this project for bridge decks. This is especially important because, as discussed later in this proposal, the thermal stresses generated in bridge decks are quite high and generally higher than most practitioners currently believe. This is especially the case for decks in Texas, where wet curing is typically applied for 8-10 days, minimizing the role

of early-age drying shrinkage and causing thermal effects to be become an even larger percentage of the early volume change. In fact, subsequent cracking frame testing of the concrete used in the bridge deck shown in Figure 3.8 confirmed that substantial thermal stresses were developed. Using ConcreteWorks as a simulation program to drive the cracking frames, additional testing was performed that clearly demonstrated and quantified the benefits of using crushed limestone, instead of river gravel, and of pouring at night, instead of during the heat of the day (see Figure 3.11). This is just one example of how useful cracking frame tests can be, especially when tied directly to a real bridge deck placement. ConcreteWorks can be an ideal tool that would allow a contractor to play "what if" games and to optimize his/her materials, mixture proportions, and construction operations to minimize early-age cracking.

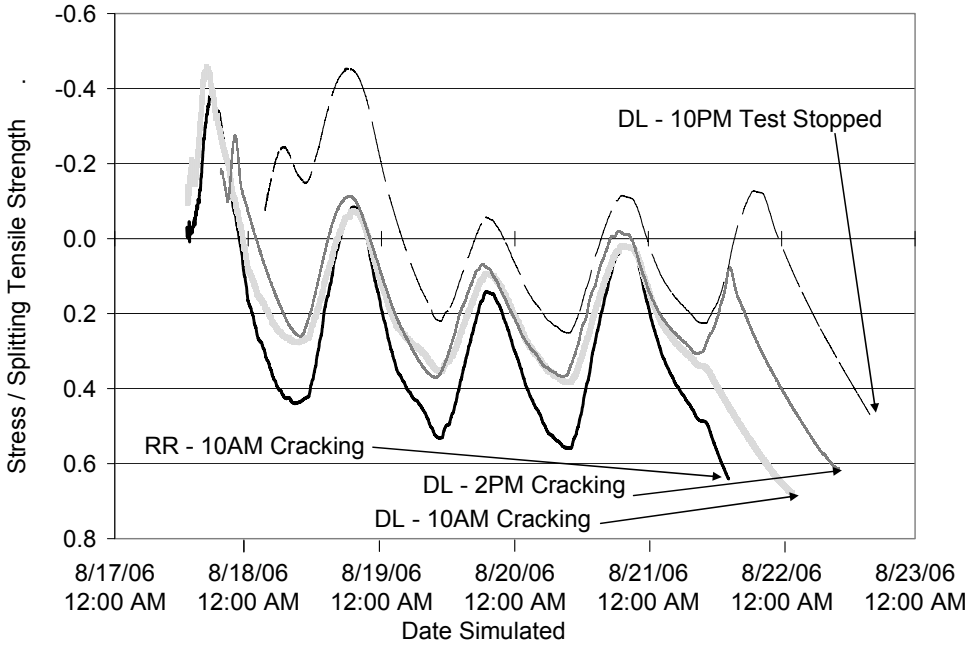

Figure 3.11: Stress development of various bridge deck mixtures (Riding et al. 2009)

Another issue that will be evaluated in Phase II will be the interplay between the moisture content (e.g., internal relative humidity) and thermal properties of concrete, and vice-versa. As mentioned in the Background section, variations in the moisture content can alter the CTE of concrete by as much as 15% (Emmanuel and Hulsey, 1977).

3.2.6 Creep and Stress Relaxation

In order to accurately predict the behavior of concrete in bridge decks, it is imperative to correctly account for the effects of creep/ stress relaxation. Ignoring such effects can lead to non-conservative calculated stresses when compressive stresses calculated are not relaxed sufficiently in the model. To successfully model creep, any model used in this program must:

- Be simple to use and have intuitive parameters that provide a simple and easily determined relationship between materials used and the parameters in the model
- Be based on creep data from the time of setting until at least several years of age

- Include the effects of drying on creep
- Not require users to run tests or require inputs or knowledge beyond the mixture proportions, compressive strength development, or project location

Traditional creep models are based on concrete compression tests performed according to ASTM C 512. In this test, the strain of a concrete cylinder is measured over a period of time after being placed in compression. In order to complete this test, the concrete must have reached a sufficient strength to de-mould and sustain a reasonable load, which usually occurs at 2 days after mixing. This test method and all models based on it completely miss the concrete creep response before the mold removal and loading. Fortunately, the research team developed a new method for calculating the concrete creep response from rigid cracking frame tests as part of project 4563. The rigid cracking frame tests are run for 96 hours, which was sufficient for modeling mass concrete stresses, but not the stresses that accumulate in bridge decks over years of drying and annual thermal cycles. A major task of this project will be to seamlessly integrate concrete creep from models of long term creep with the early age concrete creep data generated under project 4563.

A smooth transition is needed between the early age response and a long term creep model. A lot of effort has been spent by numerous researchers in developing models that can predict the long term concrete creep from the materials used. The most efficient use of resources for this project will be to use one of these models as the backbone for concrete creep model that includes early age concrete creep. This can be accomplished by adding a term to the long term creep model that is equal to zero at the time of set, and transitions to one at four days. The early age data can be added by adding a term to the long term creep model. This term will also have a time factor term that will be equal to one at setting, and transition to zero at four days, as shown in Equation 18:

$$J(t) = J_{longterm} \cdot (t) + J_{earlyage} \cdot (1 - t) \quad \text{Eq. 18}$$

where t is the time from setting, J(t) is the creep compliance function, Jlongterm is the creep compliance long term model selected, and Jearlyage is the model developed for the early age concrete creep.

There are three commonly used long term creep models which can be viewed as candidates as the base model for the new concrete lifetime creep model: the CEB-FIP model code (1993), the ACI 209 model for creep, and the B3 model by Bazant and Baweja (1995). The B3 model is rather complex to use, and the coefficients have little physical meaning making the practical implementation of a model based on the B3 model difficult. The ACI 209 model, which is commonly used in prestressed concrete calculations, is simple to use. The accuracy of the model is however not sufficient for a bridge deck stress model. The CEB-FIP model is much simpler to use than the B3 model, but is more accurate than the ACI 209 model. There are also fewer parameters in the CEB-FIP model, which will make it easier to use. The early age concrete creep data generated through previous efforts of the research team will be combined with data generated as part of this project. The early age model developed as part of project 4563 used the principle of superposition to calculate the creep response with time of the concrete, which can be computationally slow after about four days of simulated time. It is anticipated that the combined early and long term creep model that will be developed as part of this project will use Maxwell chain models instead of the principle of superposition to decrease the model runtime.

In summary, the following will be accomplished during this task:

- Combine the data generated as part of previous research work with that generated as part of this project
- Develop a numerical method for combining early and later age concrete creep model that integrates data from both rigid cracking frame and conventional ASTM C 512 creep tests
- Develop a statistical model of the early age parameters in the numerical model that will accurately predict the cracking frame creep response and the later age concrete creep

3.3 Field Evaluations

One of the most important aspects of this task will be the calibration/validation of the bridge deck heat model developed under TxDOT 4563 and refined under this project. Only minimal field monitoring and calibration was performed under TxDOT 4563, and is proposed that three to five bridge decks cast on top of precast panels/girders be instrumented and monitored, along with one to three bridge decks cast over stay-in-place metal pans (or equivalent). Based on these results, the bridge deck heat model will be improved through the calibration process, and additional data will be sought to serve as validation to this model.

In addition, some of the above bridge decks will be cast with imbedded strain gages or vibrating wire gages to track strains throughout the deck. This is somewhat challenging data to decipher as fully restrained concrete will register no strain, whereas unrestrained concrete will register strain (but no actual stress). If feasible or technically possible, the research team will attempt to use "stress gages," developed in Japan and described in RILEM, to correlate to stress predictions it should be noted that there is very little data on this technique, and it is uncertain whether it could be integrated into this project.

Lastly, the research team will attempt to calibrate/validate the maturity-based strength prediction model by procuring cores from selected bridge decks. Standard laboratory-based maturity testing will be performed using the same material and proportions that was used in the subject bridge deck as maturity is a mixture-specific parameter. In addition, Q-drum mixtures for each bridge deck will be cast and evaluated, thereby providing a direct linkage to the materials and mixture proportions used in the field trials.

3.4 Framework for Modeling Bridge Deck Cracking

Before describing the specific framework and intended approach to model bridge deck cracking, this section briefly describes how this module fits into the existing version of ConcreteWorks (V. 2.0.6) and how the model will be expanded to include the estimation of cracking risk for bridge decks.

Table 3.5 shows the current capabilities of ConcreteWorks, including the aspects of bridge deck behavior that are currently integrated into the model, and Table 3.6 highlights the required new features and components that will be developed in order to model and predict bridge deck cracking.

Table 3.5: Software features currently available within ConcreteWorks for each concrete member type (with bridge decks in bold) (Riding 2007)

Member Type		Initial Chloride Profile Input for Existing Structures	Chloride Service Life	Thermal Cracking Risk	Temperature Prediction
Mass Concrete	Rectangular Column		X	X	X
	Rectangular Footing		X	X	X
	Partially Submerged Rectangular Footing		X	X	X
	Rectangular Bent Cap		X	X	X
	T-Shaped Bent Cap		X		X
	Circular Column		X		X
	Drilled Shaft		X		X
Precast Concrete Members	Box Beam (Type 5B40)				X
	Type IV I-Beam				X
	U40 Beam				X
	U54 Beam				X
Bridge Deck Types	**Precast 1/2 Depth Panels**	**X**	**X**		**X**
	Permanent Metal Decking	**X**	**X**		**X**
	Removable Forms	**X**	**X**		**X**
	User-Defined	**X**	**X**		**X**
Pavements	User-Selected Layers				X

Table 3.6: Proposed bridge deck cracking model (with newly proposed features in shaded cells)

Bridge Deck Types	Service life prediction (corrosion triggered by external chlorides)	Temperature prediction	Cracking Risk*			
			Plastic shrinkage	Autogenous shrinkage	Drying shrinkage	Thermal shrinkage
Precast 1/2 Depth Panels	X	X				
Permanent Metal Decking	X	X				
Removable Forms	X	X				
User-Defined	X	X				

**** Overall cracking risk will take into account all types of volume changes shown below, will adjust for creep/stress relaxation, and will account for internal/external restraint.***

Given the complexity of the physical processes, the targeted bridge deck geometries, which, in general, may depart from canonical rectangular or parallelepiped shapes, the presence of various types of restraints and/or boundary conditions, the presence of the steel reinforcement, and the need to test the developed module against results produced by existing general-purpose tools, the team intends to build the module using the finite element method as the underlying solution engine. Finite differences were sufficient as an analysis tool when taking into account the relative simplicity of the shapes considered thus far in ConcreteWorks: however, for the development targeted in the present proposal, relying on finite differences will be unduly restrictive and impractical. In fact, the proposed finite element development will also allow the team to extend the existing capabilities of ConcreteWorks to now include, for example, circular column cross-sections, which have, thus far, been difficult or impossible to tackle efficiently using the finite difference engine of ConcreteWorks.

To illustrate the proposed development using finite elements, discussions follow on how the method would be used to model, for example, the stress and/or displacement/strain distribution within a bridge deck, when deformations are due to temperature and/or moisture drivers. As discussed, both moisture concentrations and temperatures drive the outlined shrinkage processes. Thus, to this end, one can consider the equations of equilibrium, of the constitutive law, and of the kinematic conditions, coupled with the thermal conduction and moisture diffusion parts. Specifically, under linear elastic assumptions, the following hold:

$$\begin{aligned} &\text{div}\ \boldsymbol{\sigma}^T + \rho\mathbf{f} = \mathbf{0} \\ &\boldsymbol{\sigma} = \mathbf{C}[\boldsymbol{\varepsilon}] - \boldsymbol{\beta}T - \zeta\gamma \\ &\boldsymbol{\varepsilon} = \frac{1}{2}\left(\nabla\mathbf{u}^T + \nabla\mathbf{u}\right) \end{aligned} \qquad \text{Eq. 19}$$

where the first of equation (19) refer to equilibrium, the second to the constitutive law, and the third to the kinematic condition, with $\boldsymbol{\sigma}$ and $\boldsymbol{\varepsilon}$ denoting the second-order stress and strain tensors, $\mathbf{C}$ the fourth-order elasticity tensor, which for the isotropic case reduces to an expression implicating just the two Lamé constants, and $\mathbf{u}$ the displacement vector (the notation

$\mathbf{C}[\boldsymbol{\varepsilon}]$ implies operation of a fourth-order on a second-order tensor, and not functional dependence). Moreover, T is temperature, γ is the change in moisture concentration, $\boldsymbol{\beta}$ and $\boldsymbol{\zeta}$ are the stress-temperature and stress-moisture tensors ($\boldsymbol{\beta} = \mathbf{C}\boldsymbol{\alpha}$, with $\boldsymbol{\alpha}$ denoting the coefficients of thermal expansion; and $\boldsymbol{\zeta} = \mathbf{C}\boldsymbol{\lambda}$, with $\boldsymbol{\lambda}$ denoting the coefficients of moisture expansion); $\mathbf{f}$ denotes body forces.

Notice that, under the working hypothesis (also built in ConcreteWorks) of quasi-static thermo-hygro-elasticity, the only coupling between stresses and temperatures/moisture concentrations appears in the constitutive law. To complete the picture of the now (loosely) coupled thermo-hygro-mechanical modeling, one needs to add the heat conduction and moisture diffusion parts, which, respectively, are described by:

$$\nabla(k\nabla T) = \rho C_v \frac{\partial T}{\partial t}$$
$$\nabla(\xi\nabla \gamma) = \frac{\partial \gamma}{\partial t} \qquad \text{Eq. 20}$$

In the above C_v is heat capacity per unit mass, and k, ξ are thermal conductivities and moisture diffusivity coefficients, respectively, which are proportional to the aforementioned thermal and moisture expansion coefficients (the latter are input by the user, and recoverable through in-situ experiments). The above equations are, of course, subject to appropriate boundary conditions, that include not only structural boundary constraints (supports, restraints, etc), but thermal and hygral as well (e.g., insulated or exposed surfaces).

We remark that the system of equations outlined above parallels the earlier development on the thermal response of mass concrete, currently implemented in ConcreteWorks. In other words, the contribution of the drying shrinkage to the cracking potential will be taken into account in a manner similar to the one the thermal shrinkage is currently accounted for, owing to the similarity of the mathematical models describing the diffusive nature of both processes. As discussed earlier in this report, the development hinges on being able to quantify the spatial distribution of the moisture diffusivity coefficients, based on the planned experiments. In this manner, both thermal and drying shrinkages will be taken into account simultaneously.

It is important to note that the formulation is general enough to accommodate both the concrete and the steel reinforcement. For example, elements accounting for the three-dimensional solids will be developed to allow for the modeling of the concrete part of the deck, whereas, one-dimensional axial elements will be included to account for the reinforcement under perfect bonding conditions.

Similar to ConcreteWorks, the heat conduction and moisture diffusion parts (Eq. 19) are solved first, driven by their respective boundary conditions, on a per time-step basis. The structural part is quasi-static, that is, it is static within each time-step, as clearly suggested by (18), whereas the temperature and moisture parts are time-dependent, as suggested by (19). Within the context of finite elements, classical Galerkin lines suggest the casting of the above equations in a, so-called, weak form, that, in turn, leads to the discrete algebraic forms upon introduction of a) discretization of the geometric domain of interest (e.g. the deck) into elements, and b) specific approximations within each element for each of the primary unknowns implicated in the above, that is, of the displacements $\mathbf{u}$, temperatures T, and moisture concentration

changes γ. The research team will likely use quadratic isoparametric elements to model the primary unknowns, thereby also allowing for curved deck geometries. There results a system of linear equations which can be subsequently solved for the primary unknowns. Secondary quantities, such as the stresses, are recovered during a post-processing step that includes differentiation of the primary quantities on a per-element basis, and the taking into account of the constitutive law and kinematic conditions. In short, the modeling steps include modules dedicated to:

- Input of material parameters
- Input of geometric parameters defining the domain of interest
- Meshing of the deck
- Imposition of boundary conditions
- Construction of the element stiffness matrices
- Assembly of the global system stiffness and force vectors
- Solution of the resulting algebraic equations
- Post-processing

Once the stress distribution is recovered, it is then possible to assess the cracking potential due to the combined effect of all shrinkages using the same rationale that was used in ConcreteWorks, that is, based on stress-threshold criteria.

The research team, led by Dr. Kallivokas, intends to provide a module capable of modeling a bridge deck corresponding to a representative bridge span, driven by user input. Modifications of the elastic moduli to account for creep could be easily incorporated into the above procedure.

Lastly, the research team intends to validate the software development in two ways: first, against results produced by general-purpose commercially available finite element packages, such as Ansys (see Fig. 3.12 for an illustrative analysis of a concrete deck subjected to thermal gradients). Secondly, validation with experimental in-situ measurements: whereas it is conceivable that one could recover moisture and temperature distributions at a given point in time, and thus compare against the software predictions, it is presently impossible to recover in-situ the stress distribution. Alternatively, strain and, more generally, deformation measurements can be used to assess the quality of the predictions.

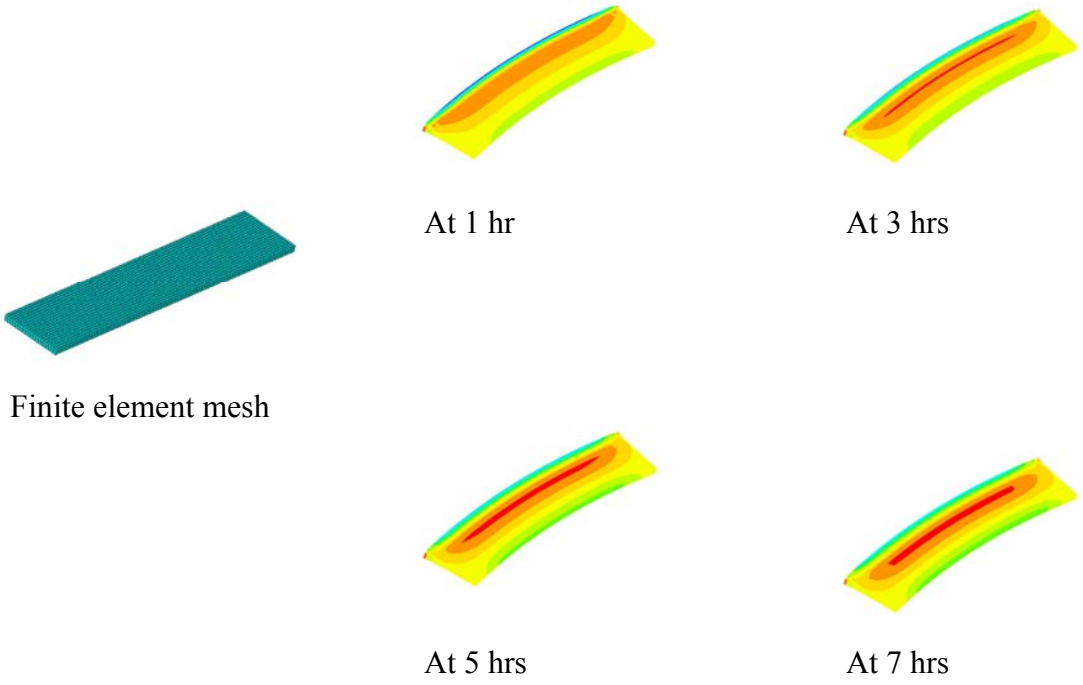

Figure 3.12: A simple span bridge deck exposed to temperature differentials on its vertical sides; longitudinal normal stress distribution, sampled at 2 hour intervals during the first 8 hours from the onset of the thermal gradients.
Note that the thermal gradient is applied from the sides strictly for illustrative purposes; actual thermal gradients in bridge decks would tend to be in the orthogonal direction.

3.5 Implementation and Training

The research team will ensure that all products developed under this project will be readily implementable by TxDOT. This has long been a trademark of Dr. Folliard's research program, which has had a strong role in revising and improving specifications, test methods, and the state of the practice in the state of Texas and throughout the United States.

The research team will develop a training course for TxDOT engineers, contractors, and other interested parties. A pilot workshop (half-day or full-day) will be presented to the project monitoring committee and other interested parties towards the end of this project (nominally the last three months).

3.6 Final Project Report

A final project report will be submitted at the conclusion of this project that will document the main findings to date, will provide recommendations related to specifications and guidelines, and will include full documentation of the model developed under this project. At the

same time that this report is submitted, the source code for the software will be submitted in a fully documented format for review and approval by TxDOT

3.7 Information Technology (IT) Deliverables to TxDOT

The main product of this project will be an updated and expanded version of ConcreteWorks, with the newly-added bridge deck cracking model. The research team will cooperate throughout the project with TxDOT IT personnel to ensure that the program is compatible with other TxDOT products and that the user's manual is sufficient to provide guidance to end users.

3.8 Assistance or Involvement by TxDOT

Assistance or involvement by TxDOT will be essential to this project, especially in the following areas:

- Instrumentation and monitoring of selected bridge decks throughout Texas.
- Development of software in format that is compatible with other TxDOT software packages.
- Assistance in planning, organizing, and conducting training courses.

References

Abel, J. and Hover, K.C, "Effect of Water/Cement Ratio on the Early Age Tensile Strength of Concrete," Transportation Research Record, Transportation Research Board, Volume 1610, 1998

ACI Building Code Committee, (2008), "Building Code Requirements for Structural Concrete (ACI 318-08) and Commentary (ACI 318R-08)," American Concrete Institute, Farmington Hills, Mi. 430 pp.

ACI Committee 209, "Prediction of Creep, Shrinkage and Temperature Effects in Concrete Structures (ACI 209R-92)," Farmington Hills, Mich., 47 pp., 1992.

ACI Committee 224, "Control of Cracking in Concrete Structures (224R-01)," Farmington Hills, Mich., 2001.

ACI Committee 305, "Hot Weather Concreting (ACI 305R-96)" *Manual of Concrete Practice*, Part 2. Farmington Hills: American Concrete Institute, 1996.

Akita, H., Fujuwara, T., Ozaka, Y. 'Practical procedure for the analysis of moisture transfer within concrete due to drying' Mag. Of Concr. Res. Vol. 49, No. 179, pp. 1-7, 1997.

Al-Fadhala, M., and Hover, K.C., "Rapid Evaporation from Freshly Cast Concrete and the Gulf Environment," Construction and Building Materials, Vol. 15, pp. 1-7, 2001.

Al-Manaseer and Jian-Ping Lam, Statistical Evaluation of Shrinkage and Creep Models, *ACI Materials Journal*, V. 102, No. 3, May-June 2005.

Altouband, Salah and Lange, David, "Creep, Shrinkage, and Cracking of Restrained Concrete at Early Age," ACI Materials Journal, V. 98, No. 4, July 1, 2001.

American Society of Civil Engineering (ASCE),"Report Card for America's Infrastructure: 2009 Progress Report", ASCE, Online at http://www.asce.org/reportcard/, 2009.

Babaei, Khossrow and Fouladgar, Amir, "Solutions to Concrete Bridge Deck Cracking," Concrete International, V. 19, No. 7, July 1 1997.

Bazant, Z.P., and Baweja, S., "Justification and refinements of model B3 for concrete creep and shrinkage 2. Updating and theoretical basis," Materials and Structures, Vol. 28, No. 8, 1995, pp. 488-495.

Bentz, D.P., "Influence of Shrinkage-Reducing Admixtures on Early-Age Properties of Cement Pastes" Journal of Advanced Concrete Technology, Vol. 4 No. 3, 423-429, 2006.

Bentz, D.P., and Jensen, O.M., "Mitigation Strategies for Autogenous Shrinkage Cracking,"

Cement and Concrete Composites, 26 (6), 677-685, 2004.

Bentz, D.P., Garboczi, E.J., Quenard, D.A., 'Modeling drying shrinkage in reconstructed porous materials: application to porous vycor glass', Modeling Simul. Mater. Sci. Eng., pp 211 236, 1998.

CEB-FIP Model Code '90, Comité Euro-International du Beton, Bulletin D'information No. 213,214, Tomas Telford, London, May 1993, 473 pp.

Darwin, D., J. and Browning, 2008, Construction of Low Cracking High Performance Concrete (LC-HPC) Bridge Decks: Field Experience, Proceedings of the Concrete Bridge Conference, May 4-7, 2008, St. Louis, MO, CD-Rom.

Emborg, M., (1998b). "Models and Methods for Computation of Thermal Stresses," In RILEM Report 15, Prevention of Thermal Cracking in Concrete at Early Ages, Edited by R. Springenschmid, E & Fn Spon, London, pp. 179-230.

Emmanuel, J.H., and J.L. Hulsey. 1977. "Prediction of the thermal coefficient of expansion of concrete," Journal of the American Concrete Institute, Vol. 74, No. 4, pp. 149-155.

Folliard, K.J., Smith, C., Sellers, G., Brown, M., and Breen, J. "Evaluation of Alternative Materials to Control Drying-Shrinkage Cracking in Concrete Bridge Decks," TxDOT Report 4098-4, 2003

Folliard, K.J., Juenger, M., Schindler, A., Riding, K., Poole, J., Kallivokas, L, Slatnick, S., Whigham, J, and Meadows, J., "Prediction Model for Concrete Behavior—Draft Final Report," TxDOT 4563, 2008.

Gardner, N. J., and Lockman, M. J., "Design Provisions for Drying Shrinkage and Creep of Normal-Strength Concrete," *ACI Materials Journal*, V. 98, No. 2, Mar.-Apr. 2001, pp. 159-167.

Grasley, Z.C., and Lange, D.A., "Modeling Drying Shrinkage Stress Gradients in Concrete," Cement, Concrete, and Aggregates, Vol. 26, No. 2, pp. 115-122, 2004.

Hedlund, H., "Hardening Concrete. Measurements and evaluation of non-elastic deformation and associated restraint stresses," Luleå, Sweden: Division of Structural Engineering, Luleå University of Technology. Doctoral Thesis 2000:25, 394 pp., December 2000.

Jensen, O.M.; and Hansen, P.F., "Autogenous deformation and RH-change in perspective," Cement and Concrete Research, V. 31, pp. 1859-1865, 2001.

Krauss, P.D., and Rogalla, E.A., "Transverse Cracking in Newly Constructed Bridge Decks," National Highway Cooperative Research Program (NCHRP) Report 380, Transportation Research Board, 1996.

Larson, M., "Thermal Crack Estimation in Early Age Concrete— Models and Methods for Practical Application," doctoral thesis, Luleå University of Technology, Division of Structural Engineering, 2003, 190 pp.

Lura, P., Jensen, O.M., and van Breugel, K., "Autogenous shrinkage in high-performance cement paste: An evaluation of basic mechanisms," Cement and Concrete Research, Volume 33, Issue 2, Pages 223-232, 2003.

Mangold, M. Methods for Experimental Determination of Thermal Stresses and Crack Sensitivity in the Laboratory. In Rilem Report 15, Prevention of Thermal Cracking in Concrete *at Early Ages*, Edited by R. Springenschmid, E & Fn Spon, London, 1998, pp. 26-39.

Muller, H. S., and Hilsdorf, H. K., "Evaluation of the Time-Dependent Behavior of Concrete, Summary Report on the Work of General Task Group 9," *CEB Bulletin d' Information*, No. 199, Sept. 1990, pp. 290.

Ono, P., "Plastic Shrinkage Cracking and Evaporation Formulas," ACI Materials Journal, July-August, 1998.

Poole, Jonathan, "Modeling Temperature Sensitivity and Heat Evolution of Concrete," Ph.D. Dissertation, The University of Texas at Austin, 2007.

Powers, T. C., *The Properties of Fresh Concrete*, John Wiley and Sons, 1968. Riding, Kyle, "Early Age Concrete Thermal Stress Measurement and Modeling," Ph.D. Dissertation, The University of Texas at Austin, 2007.

Raphael, J.M., (1984). "Tensile Strength of Concrete," ACI Journal, Vol. 81, No. 2, pp. 158-165.

RILEM Draft Recommendation, 1995, "Creep and Shrinkage Prediction Model for Analysis and Design of Concrete Structures-Model B3," Ed. Z.P. Bazant, S. Baweja, *Materials and Structures,* Vol. 28, pp. 357-365, 1995.

Schindler, A.K., "Concrete hydration, temperature development, and setting at early ages", Ph.D. Dissertation, The University of Texas at Austin, 2002.

Schindler A.K., Prediction of concrete setting. Proceedings of the RILEM International Symposium on Advances in Concrete through Science and Engineering, Edited by J. Weiss, K. Kovler, J. Marchand, and S. Mindess, RILEM Publications SARL, Illinois, 2004.

Springenschmid, R. and R. Breitenbücher. Influence of Constituents, Mix Proportions and Temperature on Cracking Sensitivity of Concrete. In *Rilem Report 15, Prevention of Thermal Cracking in Concrete at Early Ages*, Edited by R. Springenschmid, E & Fn Spon, London, 1998, pp. 40-50.

Turcry, P., Loukili, A., Laurent, B., Casabonne, J., "Can the maturity concept be used to separate the autogenous shrinkage and thermal deformation of a cement paste at early age?," Cement and Concrete Research, 2002.

Viviani, M., (2005). "Monitoring and Modeling of Construction Materials During Hardening," Doctoral Thesis, Swiss Federal Institute of Technology, Lausanne, Switzerland, 172 pp.

Whigham, J., "Evaluation of Restraint Stresses and Cracking in Early-Age Concrete with the Rigid Cracking Frame," Master's Thesis, Auburn University, 2005.

Wittmann, F.H., Roelfstra, P.E., 'Total deformation of loaded drying concrete,' *Cem. and Conc. Res.* 10 (1980) 601-610.